UNCLASSIFIED

AD NUMBER:	AD0819810

LIMITATION CHANGES

TO:

Approved for public release; distribution is unlimited.

FROM:

Distribution authorized to US Government Agencies only; Export Controlled; 1 Jul 1967. Other requests shall be referred to Metals and Ceramics Division, Air Force Materials Laboratory, Wright-Patterson AFB, OH 45433.

AUTHORITY

AFSC ltr dtd 21 Mar 1991

THIS PAGE IS UNCLASSIFIED

UNCLASSIFIED

DEPARTMENT OF DEFENSE
UNITED STATES OF AMERICA

AD NUMBER

819 810

CLASSIFICATION CHANGES

TO

FROM

AUTHORITY

WRDC/1st LTR dtd 21 MAR 89

THIS PAGE IS UNCLASSIFIED

AFML-TR-65-2
PART II, VOLUME XV

TERNARY PHASE EQUILIBRIA IN TRANSITION METAL-BORON-CARBON-SILICON SYSTEMS

PART II. TERNARY SYSTEMS

VOLUME XV. CONSTITUTION OF NIOBIUM-MOLYBDENUM-CARBON ALLOYS

E. RUDY
C. E. BRUKL
ST. WINDISCH

AEROJET-GENERAL CORPORATION

TECHNICAL REPORT AFML-TR-65-2, PART II, VOLUME XV.

JULY 1967

This document is subject to special export controls and each transmittal to foreign governments or foreign nationals may be made only with prior approval of Metals and Ceramics Division, Air Force Materials Laboratory, Wright-Patterson Air Force Base, Ohio.

AIR FORCE MATERIALS LABORATORY
RESEARCH AND TECHNOLOGY DIVISION
AIR FORCE SYSTEMS COMMAND
WRIGHT-PATTERSON AIR FORCE BASE, OHIO

NOTICES

400 - August 1967 - CO455 - 4-75

TERNARY PHASE EQUILIBRIA IN TRANSITION METAL-BORON-CARBON-SILICON SYSTEMS

PART II. TERNARY SYSTEMS

VOLUME XV. CONSTITUTION OF NIOBIUM-MOLYBDENUM-CARBON ALLOYS

E. RUDY
C. E. BRUKL
ST. WINDISCH

This document is subject to special export controls and each transmittal to foreign governments or foreign nationals may be made only with prior approval of Metals and Ceramics Division, Air Force Materials Laboratory, Wright-Patterson Air Force Base, Ohio.

FOREWORD

The research described in this report was carried out at the Materials Research Laboratory, Aerojet-General Corporation, Sacramento, California, under USAF Contract No. AF 33(615)-1249. The contract was initiated under Project No. 7350, Task No. 735001, and was administered under the direction of the Air Force Materials Laboratory, Research and Technology Division with Lt. P.J. Marchiando acting as Project Engineer, and Dr. E. Rudy, Aerojet-General Corporation, as Principal Investigator. Professor Dr. Hans Nowotny, University of Vienna, served as consultant to the project.

The project, which includes the experimental and theoretical investigations of ternary and related binary systems in the system classes Me_1-Me_2-C, Me-B-C, Me_1-Me_2-B, Me-Si-B and Me-Si-C, was initiated on 1 January 1964. An extension effort to this contract commenced in January 1966.

The phase diagram work on the ternary system described in this report, was carried by E. Rudy, C. Brukl, and St. Windisch. Assisting in the investigations were: J. Hoffman (metallographic preparations), J. Pomodoro (sample preparation), and R. Cobb (X-ray exposures and photographic work).

Chemical analysis of the alloys was performed under the supervision of Mr. W.E. Trahan, Quality Control Division of Aerojet-General Corporation. The authors wish to thank Mr. R. Cristoni for the preparation of the illustrations, and Mrs. J. Weidner, who typed the report.

The manuscript of this report was released by the authors March 1967 for publication as an RTD Technical Report.

Other reports issued under USAF Contract AF 33(615)-1249 have included.

Part I. Related Binaries

Volume I.	Mo-C System
Volume II.	Ti-C and Zr-C Systems
Volume III.	Systems Mo-B and W-B
Volume IV.	Hf-C System
Volume V.	Ta-C System. Partial Investigations in the Systems V-C and Nb-C
Volume VI.	W-C System. Supplemental Information on the Mo-C System
Volume VII.	Ti-B System
Volume VIII.	Zr-B System
Volume IX.	Hf-B System
Volume X.	V-B, Nb-B, and Ta-B Systems
Volume XI	Final Report on the Mo-C System

Part II. Ternary Systems

Volume I.	Ta-Hf-C System
Volume II.	Ti-Ta-C System

FOREWORD (Cont'd)

Volume III.	Zr-Ta-C System
Volume IV.	Ti-Zr-C, Ti-Hf-C, and Zr-Hf-C Systems
Volume V.	Ti-Hf-B System
Volume VI.	Zr-Hf-B System
Volume VII.	Systems Ti-Si-C, Nb-Si-C, and W-Si-C
Volume VIII.	Ta-W-C System
Volume IX.	Zr-W-B System. Pseudo-Binary System TaB_2-HfB_2
Volume X.	Systems Zr-Si-C, Hf-Si-C, Zr-Si-B, and Hf-Si-B
Volume XI.	Systems Hf-Mo-B and Hf-W-B
Volume XII.	Ti-Zr-B System
Volume XIII.	Phase Diagrams of the Systems Ti-B-C, Zr-B-C, and Hf-B-C
Volume XIV.	The Hafnium-Iridium-Boron System

Part III. Special Experimental Techniques

Volume I.	High Temperature Differential Thermal Analysis
Volume II.	A Pirani-Furnace for the Precision Determination of the Melting Temperatures of Refractory Metallic Substances

Part IV. Thermochemical Calculations

Volume I.	Thermodynamic Properties of Group IV, V, and VI Binary Transition Metal Carbides.
Volume II.	Thermodynamic Interpretation of Ternary Phase Diagrams
Volume III.	Computational Approaches to the Calculation of Ternary Phase Diagrams.

This technical report has been reviewed and is approved.

W. G. RAMKE
Chief, Ceramics and Graphite Branch
Metals and Ceramics Division
Air Force Materials Laboratory

ABSTRACT

The ternary alloy system niobium-molybdenum-carbon was investigated by means of X-ray, melting point, DTA, and metallographic techniques; a complete phase diagram for temperatures above 1500°C was established.

Above 1960°C, niobium monocarbide and the cubic (B1) high temperature phase in the molybdenum-carbon system form an uninterrupted series of solid solutions. The ternary range of the pseudo-cubic $\eta\text{-Mo}_{1-x}$ is very restricted. Dimolybdenum carbide dissolves up to 44 mole percent Nb_2C (2240°C), whereas the maximum solid solubility of Mo_2C in Nb_2C does not exceed 5 mole percent. The order-disorder transformation temperatures in Mo_2C and Nb_2C are lowered by the mutual metal exchanges.

Six isothermal reactions occur in the ternary system; three correspond to class II-type four-phase reactions involving a liquid phase, one to a class I (eutectoid)-type, and two further isotherms are associated with limiting tie lines.

The results of the phase diagram investigation are discussed, and the thermodynamic interpretation identifies the low relative stability of the binary subcarbides in conjunction with the large stability differences between niobium and molybdenum carbides as the cause for the formation of a stable equilibrium between the monocarbide and the metal phase in the ternary region.

This document is subject to special export controls, and each transmittal to foreign governments or foreign nationals may be made only with prior approval of Metals and Ceramics Division, Air Force Materials Laboratory, Wright-Patterson Air Force Base, Ohio.

TABLE OF CONTENTS

PAGE

I. INTRODUCTION AND SUMMARY 1
  A. Introduction 1
  B. Summary 2
II. LITERATURE REVIEW 8
III. EXPERIMENTAL 10
  A. Starting Materials and Alloy Preparation 10
  B. Determination of Melting Temperatures and Differential-Thermoanalytical Studies 12
  C. Metallographic, X-Ray, and Chemical Analysis 13
IV. RESULTS 16
  A. The Niobium-Molybdenum Binary System 16
  B. Solid State Equilibria in the Ternary Nb-Mo-C System . 17
  C. Phase Equilibria at High Temperatures 24
  D. Assembly of the Phase Diagram 39
V. DISCUSSION 49

References 66

LIST OF ILLUSTRATIONS

FIGURE PAGE

1. Proposed Constitution Diagram for the Niobium-Molybdenum-Carbon System 4
2. Scheil-Schulz Reaction Diagram for Ternary Nb-Mo-C Alloys 5
3. Liquidus Projections in the Nb-Mo-C System 6
4. Isopleth at $NbC_{0.46}$-$MoC_{0.46}$. 7
5. Melting Temperatures of Niobium-Molybdenum Alloys 16
6. Lattice Parameters of the Niobium-Molybdenum Solid Solution 17
7. Qualitative X-ray and Metallographic Phase Evaluation of the Alloys Equilibrated at 1500°C 18
8. Lattice Parameters of the Cubic Monocarbide Solution Along the Section $NbC_{0.82}$-$MoC_{0.82}$, and Phase Boundary Values at 1500°C and 1900°C. 20
9. Qualitative X-Ray and Metallographic Phase Evaluation of the Alloy Series Equilibrated at 2200°C 21
10. Lattice Parameters of Monocarbide Alloys 22
11. Lattice Parameters of the Mo_2C Solid Solution 23
12. Temperatures (Bottom) and Location (Top) of the Metal-Rich Eutectic Trough in the Nb-Mo-C System 24
13. Nb-Mo-C (85-5-10 At.%), Rapidly Cooled from 2350°C 25
14. Nb-Mo-C (26-60-14 At.%), Rapidly Cooled from 2280°C 26
15. Mo-C (17 At.% C), Cooled at 14°C per Second from 2220°C 26
16. Melting and Qualitative Phase Evaluation of Alloys Located on the $\underset{\sim}{\mathrm{Nb}}_2\mathrm{C}$-$\underset{\sim}{\mathrm{Mo}}_2\mathrm{C}$ Section. 28
17. DTA-Thermograms of the Two Ternary Alloys Participating in Four-Phase Reactions. 29
18. Nb-Mo-C (59-8-33 At.%), Cooled at Approximately 50°C per Second from 2650°C 30
19. Nb-Mo-C (56-12-32 At.%), Rapidly Cooled from 2600°C 30
20. Nb-Mo-C (31-36-33 At.%), Cooled at Approximately 10°C per Second from 2700°C 31

LIST OF ILLUSTRATIONS (Cont'd)

FIGURE PAGE

21. Maximum Solidus Temperatures of the Cubic Monocarbide Phase 33

22. Nb-Mo-C (28-25-47 At.%), Quenched from 3260°C. 34

23. Nb-Mo-C (40-18-42 At.%), Melted at 3250°C, Reequilibrated for 15 Minutes at 3000°C and Quenched 35

24. Experimental Solidus Temperatures (Bottom) and Location of the Eutectic Trough (Top) Between the Monocarbide Solution and Graphite 37

25. Nb-Mo-C (34-10-56 At.%), Cooled at Approximately 100°C per Second from 3250°C 38

26. Nb-Mo-C (20-30-50 At.%), Cooled at Approximately 100°C per Second from 3000°C 38

27. Nb-Mo-C (3-52-45 At.%), Cooled at Approximately 40°C per Second from 2500°C. 39

28(a) through 28(h). Isothermal Sections for the Nb-Mo-C System 40

28(a): 1500°C
28(b): 1900°C
28(c): 2240°C
28(d): 2325°C
28(e): 2540°C
28(f): 2600°C
28(g): 2640°C
28(h): 3000°C

29(a) through 29(c). Free Enthalpy of Formation — Concentration Gradients for Niobium-Molybdenum-Alloys and Solutions of Niobium-Molybdenum Carbides 57

29(a): 1800°K
29(b): 2100°K
29(c): 2500°K

30. Calculated Integral Free Enthalpies for the Disproportionation of the Solid Solution $(Nb, Mo)_2C$ into (Nb, Mo) and $(Nb, Mo)_{1-x}$ Solid Solutions 60

31(a) through 31(c). Calculated Temperature Sections for the Nb-Mo-C System. 62

31(a): 1800°K
31(b): 2100°K
31(c): 2500°K

LIST OF TABLES

TABLE		PAGE
1	Structure and Lattice Parameters of Niobium and Molybdenum Carbides	9
2	Carbon Analyses and Lattice Parameters of Carbide Starting Materials	11
3	Etching Procedures for Nb-Mo-C Alloys	14
4	Free Enthalpy Data of Niobium Carbides ($T > 1500°C$)	54
5	Free Enthalpy Data of Molybdenum-Carbides ($T > 1500°C$)	55

I. INTRODUCTION AND SUMMARY

A. INTRODUCTION

Due to their refractoriness, the carbides of the high melting transition metals have received increased interest in recent years as base materials in composite structures for aerospace application at high temperatures; other novel fields of application include power reactors, where operation at high temperatures becomes essential for attaining high power efficiencies.

Unlike traditional uses of carbides, such as in cutting tools and abrasion-resistant linings, where overall temperatures above a few hundred degrees centigrades are seldomly encountered, the increased reaction rates at temperatures approaching melting require a close consideration of the chemical interactions between the alloy constituents. As a consequence, a detailed knowledge of the phase-relationships in the alloy systems is required in order to provide a sound basis for developmental-type work.

Partly as a result of the considerable experimental difficulties associated with the investigation of this high melting alloy class, no complete studies of ternary metal-carbon systems have been performed until recently. Even the high temperature phase relationships in the binary transition metal-carbon systems have been delineated only during the past few years to a degree of accuracy required for a more detailed study of ternary or higher order alloys.

In recent investigations of binary and ternary systems of refractory transition metals with carbon, boron, and silicon(1), alloys from the ternary systems Nb-Mo-C became of interest because of the demonstrated possibility(2, 3) of obtaining composites based on metal + monocarbide combinations. In the meantime, however, studies in other related ternary metal-carbon systems, such as tantalum-tungsten-carbon, have shown that the solid state equilibria may change significantly towards higher temperatures

(>2000°C), and that extrapolation based on low temperature equilibrium data are, in general, not very reliable. Thus, using the aforementioned system Ta-W-C as an example, it could be observed, that the monocarbide + metal solution is stable only at temperatures below 2450°C.

Although the lower temperature (<2000°C) phase relationships in the Nb-Mo-C system are similar to those found in Ta-W-C, a cursory thermodynamic analysis of the equilibria indicated(4) that complete solid solution formation between Mo_2C and Nb_2C should not occur at higher temperatures. The present work was conducted in order to experimentally verify these expectations and, in addition, to provide phase equilibrium data in the melting range of the alloys.

B. SUMMARY

The phase relationships in the ternary alloy system niobium-molybdenum-carbon are summarized as follows:

Above 1960°C, the cubic monocarbides NbC and α-MoC_{1-x} form a complete series of solid solutions. The lattice parameter variation shows a slight positive deviation with respect to a linear relationship between the values of the boundary phases (a = 4.470 Å for $NbC_{0.97}$; a = 4.268 Å for $MoC_{0.70}$). The maximum solidus temperatures increase smoothly from 2600°C for the binary α-MoC_{1-x}-phase at 42 At.% C to 3613°C for the niobium monocarbide at 44 At.% C.

Solid solution formation between the subcarbide phases is incomplete at all temperatures below melting. At 2240°C, dimolybdenum carbide (a = 2.990 Å, c = 4.728 Å at 30 At.% C) dissolves a maximum of 44 mole percent Nb_2C (a = 3.041 Å, c = 4.816 Å), whereas the maximum solubility in Nb_2C does not exceed 5 mole percent Mo_2C at 2325°C (a = 3.125 Å, c = 4.965 Å for Nb_2C; a = 3.108 Å, c = 4.930 Å for the solid solution at the three-phase boundary). The order-disorder transition temperatures in Nb_2C and Mo_2C are lowered by the mutual metal exchange. Both subcarbide solutions are restricted by an equilibrium Me_2C-ss + MeC-ss + Me-ss towards the ternary phase field, and the equilibrium between the monocarbide and the metal solution remains stable up to melting temperatures. The ternary range of existence of the hexagonal η-MoC_{1-x}-phase is very restricted.

Six isothermal reactions occur in the ternary region in the range from melting to 1500°C; three correspond to class II-type four-phase reactions involving a liquid phase, one to a class I (eutectoid)-type, and two further isotherms are associated with limiting tie lines. These reaction isotherms, in order of decreasing temperatures, are:

1. 2640°C: L + (Nb, Mo)C_{1-x}-ss ⟶ Mo_2C-ss
2. 2520°C: L + (Nb, Mo)C_{1-x}-ss ⟶ Mo_2C-ss + η-MoC_{1-x}-ss
3. 2400°C: Nb_2C_{1+x}-ss (disordered) ⟶ Nb_2C_{1-x}-ss (ordered) + (Nb,Mo)C_{1-x}-ss
4. 2325°C: L + (Nb, Mo)C_{1-x}-ss ⟶ Nb_2C-ss + (Nb, Mo)-ss
5. 2240°C: L + (Nb, Mo)C_{1-x}-ss ⟶ Mo_2C-ss + (Nb, Mo)-ss
6. 1550°C: η-MoC_{1-x}-ss ⟶ (Nb, Mo)C_{1-x}-ss + Mo_2C-ss + C

The isometric view of the entire phase diagram, shown for temperatures above 1500°C (Figure 1), is supplemented by a Scheil-Schultz Diagram of the binary and ternary isothermal reactions (Figure 2); the liquidus projections (Figure 3), and an isopleth, depicting the principal phase equilibria in the metal-rich portion of the system (Figure 4).

Based on existing thermochemical data for the binary metal carbides, the phase relationships were thermodynamically analyzed, and the calculated equilibria were found to be in good agreement with the experimental observations.

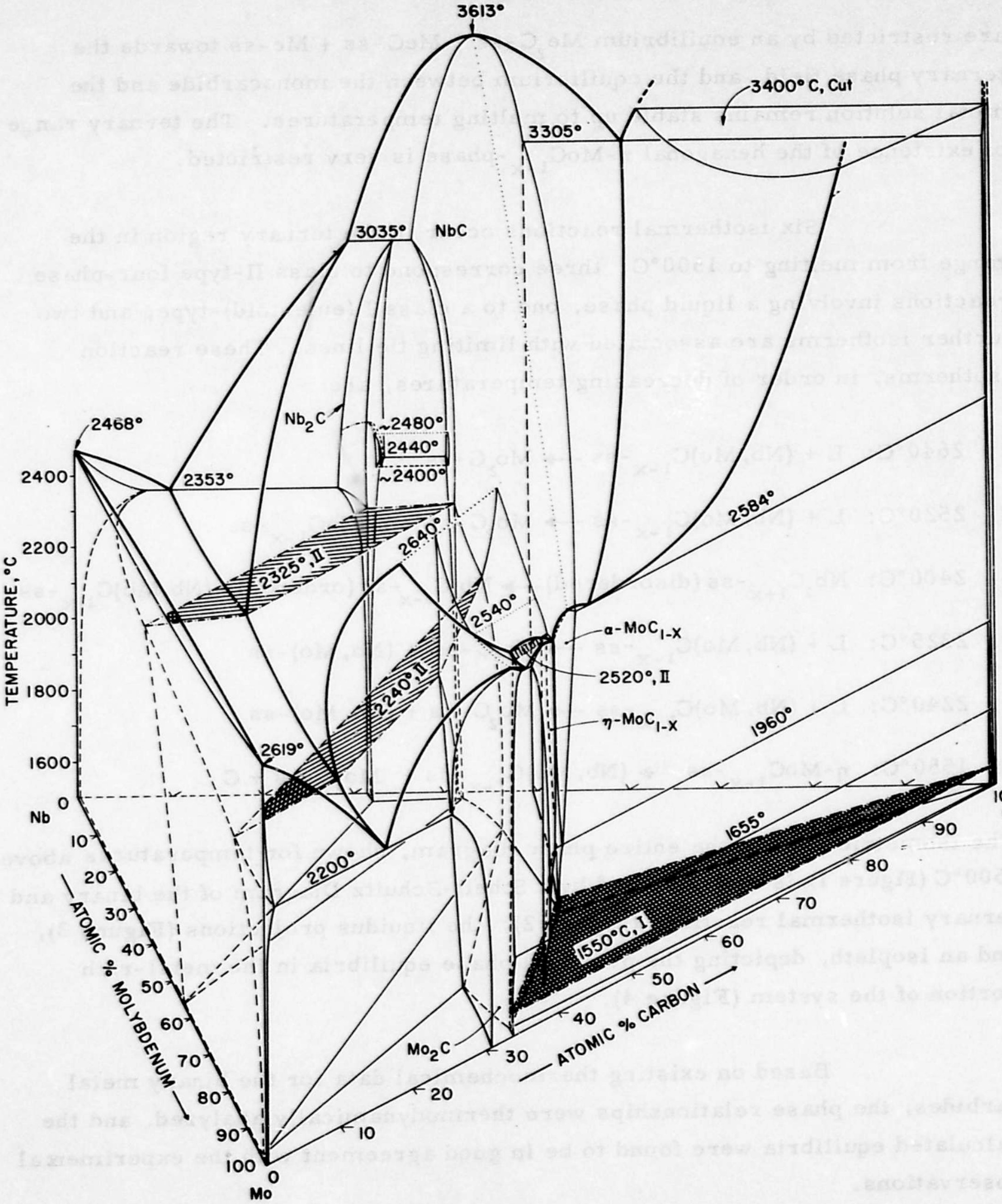

Figure 1. Proposed Constitution Diagram for the Niobium-Molybdenum-Carbon System.

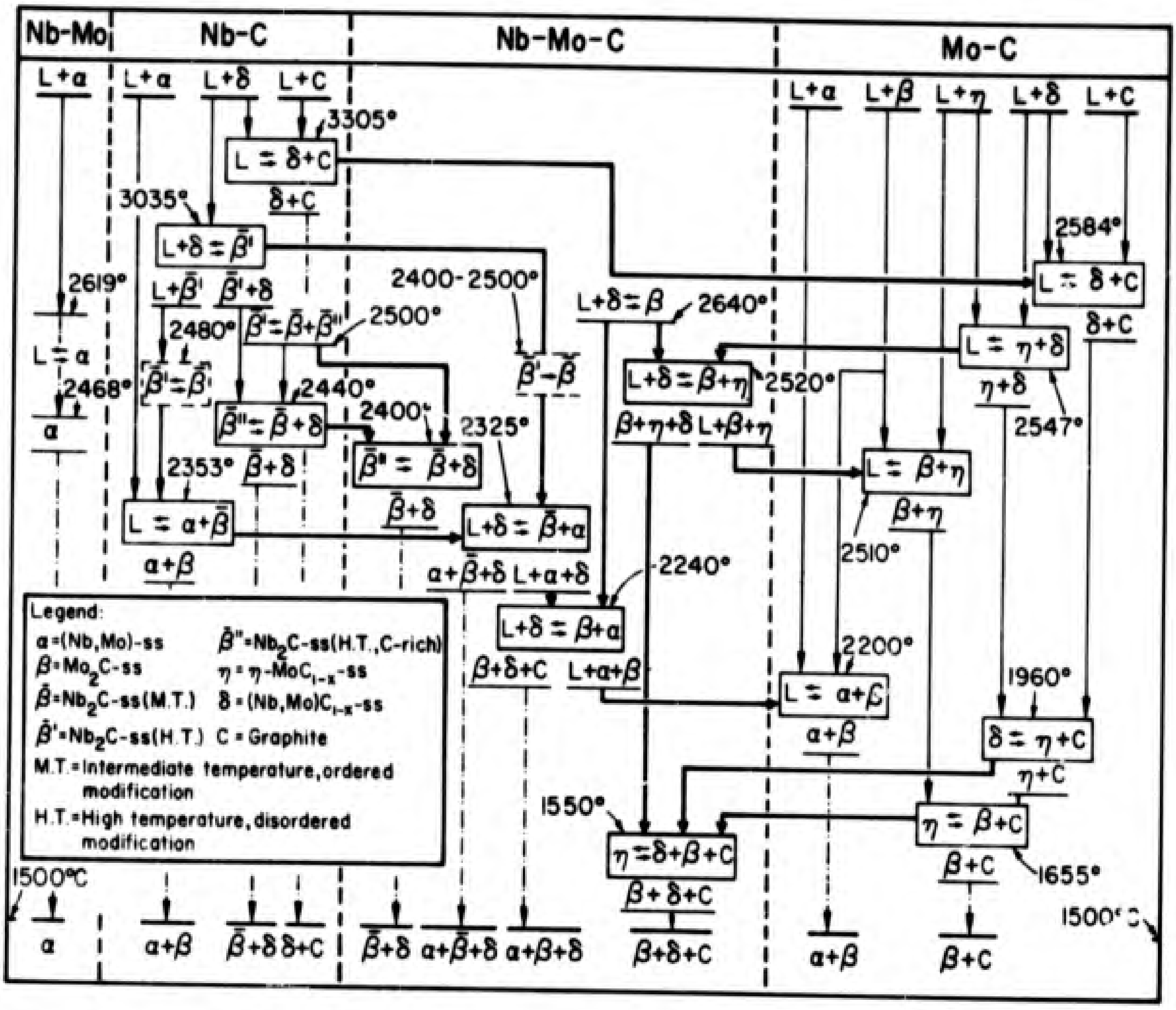

Figure 2. Scheil-Schulz Reaction Diagram for Ternary Nb-Mo-C Alloys.

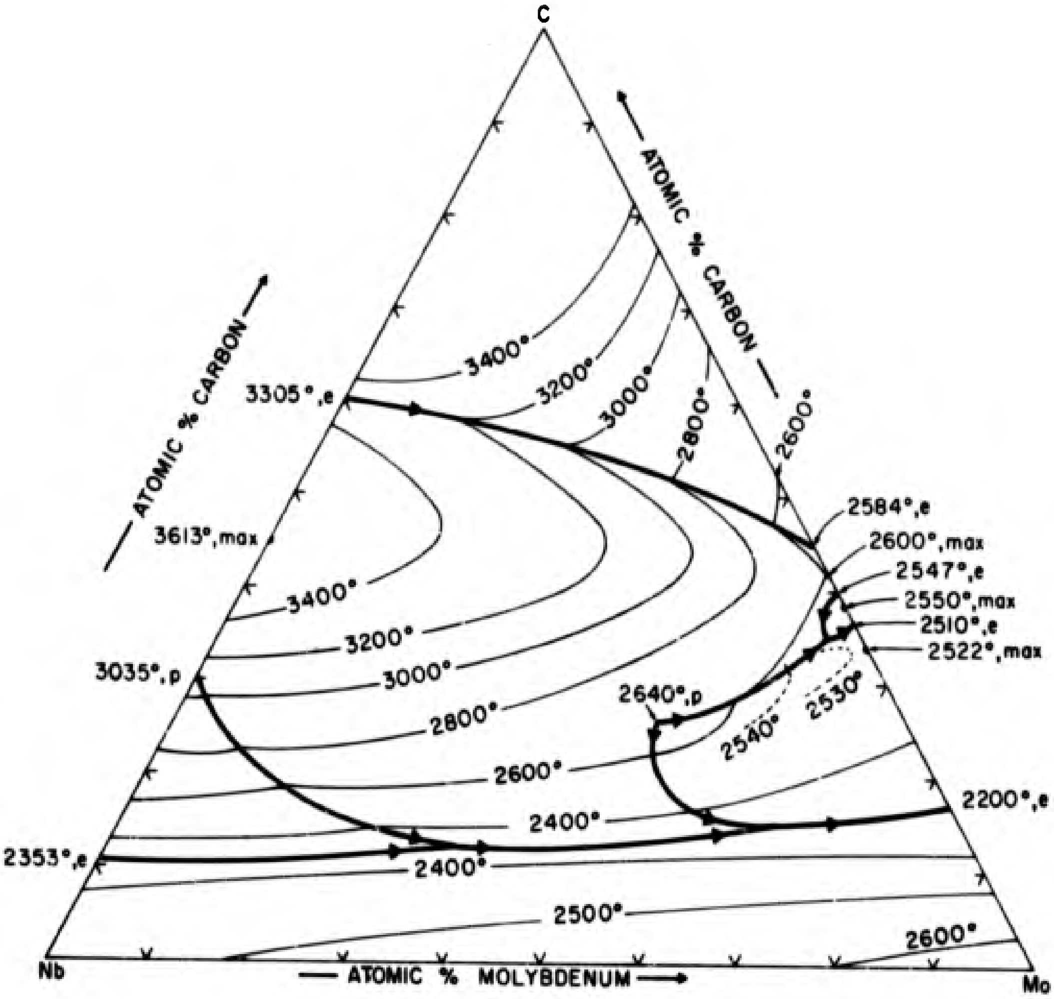

Figure 3. Liquidus Projections in the Nb-Mo-C System.

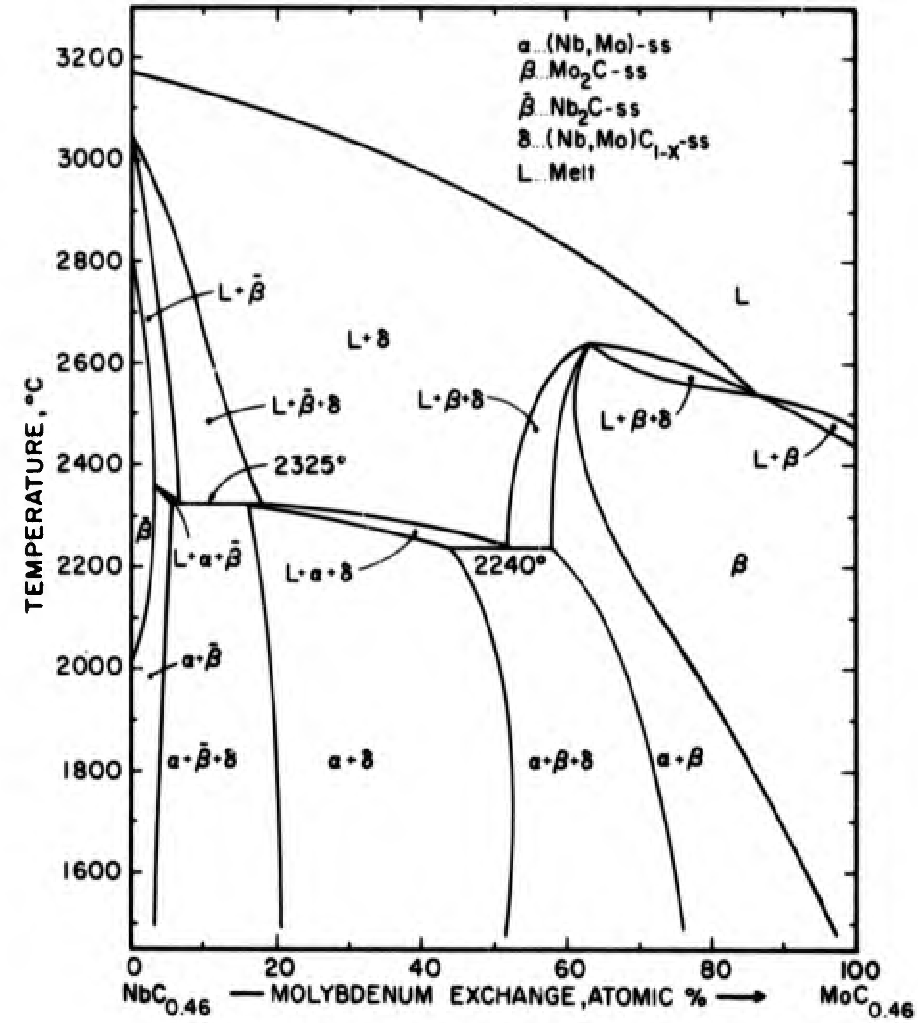

Figure 4. Isopleth at $NbC_{0.46}$-$MoC_{0.46}$.

II. LITERATURE REVIEW

In the boundary systems, niobium and molybdenum are known to form a continuous series of solid solutions(5, 6). The continuous solubility was also confirmed by I. I. Kornilov and R.S. Polyakova(7, 8), who also observed a minimum melting point at 22 At.% molybdenum and 2345°C.

The phase diagram investigations of the niobium-carbon system by E. K. Storms and N. H. Krikorian(8) and H. Kimura and Y. Sasaki(10) were recently supplemented by E. Rudy et al.(11, 12). The system contains a high melting monocarbide with the B1-structure (Table 1) and a subcarbide, Nb_2C, which exists in at least two different states of sublattice order at low temperatures(4, 11, 12, 13), and a disordered state above approximately 2500°C(11, 12). The melting point measurements by E. Rudy et al.(11, 14) are in close confirmation of the data by H. Kimura and Y. Sasaki(10).

The rather complex phase relationships in the molybdenum-carbon system were only recently clarified(15, 16). The system is characterized by three congruently melting, intermediate phases, Mo_2C, η-MoC_{1-x}, and α-MoC_{1-x} (Table 1), of which only Mo_2C is stable at temperatures below 1650°C. Substoichiometric Mo_2C exists in several states of sublattice order which interconvert in homogeneous lattice transitions. Hyperstoichiometric compositions cannot exist in the ordered state. Upon cooling through a critical temperature range, the stoichiometric carbide separates into two phases: An understoichiometric alloy which is ordered, and any hyperstoichiometric phase, which is disordered and decomposes at 1190°C into the ordered modification and elemental graphite.

Earlier investigations of ternary Nb-Mo-C alloys include the work of H. Nowotny and R. Kieffer(17), who first established the existence of extended solid solubility along the section NbC-Mo_2C, and the investigation of a temperature section of the system at 1900°C by E. Rudy et al.(2).

Table 1. Structure and Lattice Parameters of Niobium and Molybdenum Carbides

Phase	Structure	Lattice Parameters, Ångstrom
Nb_2C	1. T < 1200°C. Orthorh.	a=12.36 Å, b=10.85$_5$ Å, c=4.968 (4, 12)$^{(*)}$ a=10.92 Å, b=4.974 Å, c=3.090 Å (18) $^{(**)}$
	2. 1200-2500°C Probably hex., ε-Fe_2N-type	a=5.40$_7$ Å, c=4.960 Å (13)$^{(***)}$
	3. T > 2500°C. Hex. approaching L'3-type	a=3.127 Å c=4.972 Å at 33.3 At.% C (9)
NbC	fcc., B1-type	a=4.431 at 41.5 At.% C a=4.470 at ~50 At.% C (20)
Mo_2C	1. T < 1400°C Orthorh., D_{2h}^{14} - Pbcn	a=4.724; b=6.004; c=5.19 (21)$^{(****)}$ a=4.733; b=6.042; c=5.202 (16)
	2. T > 1400°C Hex., approaching L'3-type	a=2.990 Å, c=4.730 Å, at 30 At.% C a=3.010 Å, c=4.778 Å at 34.4 At.% C (16) (alloys quenched from 2000°C)
η-MoC_{1-x}	Hex., D_{6h}^{4}-type	a=3.006; c=14.64 (19) a=3.010; c=14.64 at 39 At.% C (16)
α-MoC_{1-x}	fcc., B1-type	a=4.266 Å at 39.7 At.% C a=4.281 Å at 43 At.% C (16)

* The orthorhombic axes are related to the (distorted) hexagonal subcell by: $a_{o.r.} \sim 4a_{hex}$; $b_{o.r.} \sim 2a_{hex}\sqrt{3}$; $c_o = c_{hex}$

** $a_{o.r.} \simeq 2a_{hex}\sqrt{3}$; $b_{o.r.} \quad c_{hex}$; $c_{o.r.} \simeq a_{hex}$

*** $a = a_{hex.\ subcell}\sqrt{3}$; $c = c_{subcell}$

**** $a_{o.r.} = c_{hex}$; $b_{o.r.} \simeq 2a_{hex}$; $c_{o.r.} \simeq a_{hex}\sqrt{3}$

III. EXPERIMENTAL

A. STARTING MATERIALS AND ALLOY PREPARATION

The elemental powders, as well as specially prepared master alloys consisting of Nb_2C, NbC, Mo_2C, and η-Mo_{1-x}, served as the starting materials for the preparation of the experimental alloys. Dimolybdenum carbide and Nb_2C were specifically used for the preparation of alloys located along the section Nb_2C-Mo_2C since the subcarbides form rather slowly, and only incompletely, when prepared from monocarbide and metal powders.

The molybdenum powder (Wah Chang Corporation, Albany, Oregon) had the following impurities after an additional hydrogen reduction at 1000°C (contents in ppm): O-160, Si-<180, N-<20, C-190, Fe+Ni+Co-<110, sum of other metallic impurities (Al, Cr, Cu, Mg, Mn, Pb, Sn, W, Ti)-<600. The overall purity of this starting material was better than 99.85%, and a lattice parameter of $a = 3.1474 \pm 0.0002$ Å was obtained from a CuK_α powder pattern.

The impurities in the niobium powder (>99.8% Nb, Wah Chang Corporation, Albany, Oregon) were as follows (in ppm): O-<420, N-<90, C-30, Ta-400, Zr-200, and the sum of other metallic impurities-<400. A lattice parameter of $a = 3.3006 \pm 0.0007$ Å, obtained from a powder exposure with Cu-K_α radiation, is consistent with parameters given in the literature(18) for high purity niobium.

The spectrographic-grade graphite powder was purchased from Union Carbide Corporation, Carbon Products Division. The total impurity content was below 2 ppm; lattice parameters of $a = 2.463$ Å, and $c = 6.729$ Å were determined from a powder pattern taken with Cu-K_α radiation.

The carbide master alloys were prepared by reacting the carefully blended and cold-compacted mixtures of the metal powders and carbon in a graphite-element furnace under a vacuum of better than 2 x 10^{-5} Torr. The reaction times used were between four to six hours; temperatures of 2100°C and 1900°C were employed for the niobium and the molybdenum carbides, respectively. The resulting reaction lumps were crushed and ball-milled under helium to a grain size smaller than 60 microns. In order to remove traces of cobalt picked up from the carbide-lined ball mill jars, the powders were leached in a hot 2N mixture of hydrochloric and sulfuric acid, washed with ether, centrifuged, and then dried under vacuum. The chemical and X-ray analyses of the carbide powders are listed in Table 2.

Table 2. Carbon Analyses and Lattice Parameters of Carbide Starting Materials

Carbide	Carbon Content At.% C	Phases Present	Lattice, Parameters, Å
Nb_2C	33.2 ± 0.2	Nb_2C + trace monocarbide	a = 3.124; c = 4.963
NbC	49.2 ± 0.2	NbC	4.470
Mo_2C	32.8 ± 0.3	Mo_2C + trace graphite	a = 4.733; b = 6.036; c = 5.205
η-MoC_{1-x}	38.4 ± 0.3	Mo_2C + C + η-MoC_{1-x} decomposition mixture	-

The majority of the ternary alloys were prepared by short duration hot-pressing(15) of the carefully blended powders in graphite dies at temperatures varying between 1800 and 2300°C. After hot-pressing, the graphite-contaminated surface zone, which was typically about 0.2 mm thick, was removed by grinding, and the cores of the samples subjected to the further homogenization treatments.

Excess metal-containing alloys were prepared by cold-pressing and subsequent sintering of the alloy compacts under vacuum (<2 x 10^{-5} Torr) at temperatures between 1600 and 2200°C. Melting point samples for the binary alloy system niobium-molybdenum were machined from electron-beam molten stock. A limited number of samples were also melted under high purity helium in a non-consumable electrode arc furnace. Altogether, approximately 380 alloys were prepared for the investigation of the ternary system.

The homogenization treatments were carried out in a tungsten mesh element furnace manufactured by the R. Brew Company. Major equilibration temperatures were: 1500°C (5×10^{-6} Torr, 140 hrs), 1900°C (10^{-5} Torr, 50 hrs), and 2200°C (1 atm He, 16 hrs). To achieve rapid cooling conditions for the alloy series treated under vacuum, helium was admitted to the furnace chamber immediately after the power had been shut off.

Apart from alloys located in the monocarbide region, where attainment of equilibrium at 1500°C could only be achieved after adding small amounts of ($\sim$ 0.1 Wt.%) cobalt to the powder mixture prior to hot-pressing, the X-ray patterns of the majority of specimens were sharp after the heat-treatments.

The change of certain equilibria with temperature was studied on alloys which were either equilibrated and then cooled at controlled rates in the DTA-apparatus, or for phase studies at temperatures close to melting, homogenized in the Pirani-furnace and then quenched in tin.

B. DETERMINATION OF MELTING TEMPERATURES AND DIFFERENTIAL-THERMOANALYTICAL STUDIES

Melting temperatures of approximately 90 ternary alloys were measured using the method devised by M. Pirani and H. Alterthum(23). In this technique, the temperature of the sample is measured by a disappearing-filament type pyrometer aimed at a small hole, generally in the order of 0.6 to 1 mm in diameter and 4 to 6 mm deep, which is located in the center of a narrowed portion of the bar-shaped specimen. Design details concerning the apparatus in use at this laboratory, as well as temperature calibration and correction procedures, have been described elsewhere(24) and therefore need not be treated at length here.

Differential thermoanalytical studies(25) were carried out on 30 ternary alloys. Tantalum monocarbide as well as carefully annealed graphite served as comparison standards. All experiments were performed using graphite containers, and the thermal behavior of each specimen was studied at controlled heating and cooling rates between 0.5°C and 18°C per second. As a result of the high solidus temperatures between niobium-rich monocarbide alloys and graphite, along with the observation, that carburization occurs rather preferentially with respect to niobium, the DTA measurements on metal-rich (< 40 At.% C) alloys could be extended to fairly high temperatures without noticeable interference from the container. All DTA specimens were sectioned and analyzed chemically and by X-rays after the runs.

Additional thermal analytical studies, covering the temperature range inaccessible by the DTA-technique described above, were carried out using a containerless heating technique(16). However, as no additional results were gained in these studies, no further reference to these experiments will be made.

C. METALLOGRAPHIC, X-RAY, AND CHEMICAL ANALYSIS

Microscopic examinations of melted as well as homogenized and quenched alloys were extensively used to locate the eutectic troughs and the homogeneity boundaries of the phases. For the metallographic studies, the specimens were mounted in a mixture of diallylphtalate and lucite-coated copper powder and preground on silicon-carbide papers of various degrees of coarseness. They were polished on microcloth using a slurry of Linde "B" alumina (0.05μ) in 5% chromic acid solution. The etching procedures varied with the composition of the alloys; they are described in Table 3.

Carbon in the alloys was determined in the well-known manner by combustion and conductometric analysis of the gas mixture. For the determination of elemental carbon, the powdered carbides first were dissolved in a mixture of nitric and hydrofluoric acid. The residual graphite

Table 3. Etching Procedures for Niobium-Molybdenum-Carbon Alloys

Alloys from the Composition Area	Etching Procedure
$Nb-Nb_{0.3}Mo_{0.7}-Nb_{0.3}Mo_{0.5}C_{0.2}-Nb_{0.8}C_{02}$	Electroetched in 0.5% oxalic acid solution
$Nb_{0.3}Mo_{0.7}-Mo-Mo_{0.6}C_{0.4}-Nb_{0.3}Mo_{0.3}C_{0.4}$	Swab-etched with 10% Murakami's(*) solution
$Nb_{0.8}C_{0.2}-Nb_{0.3}Mo_{0.5}C_{0.2}-Nb_{0.3}Mo_{0.3}C_{0.4}-Nb_{0.6}C_{0.4}$	Electroetched in 0.5% oxalic acid + dip-etched in 10% acid solution(**)
$Nb_{0.6}C_{0.4}-Mo_{0.6}C_{0.4}-Mo_{0.48}C_{0.52}-Nb_{0.48}C_{0.52}$	Dip-etched in 10% acid solution(**)
$Nb_{0.48}C_{0.52}-Mo_{0.48}C_{0.52}-C$	Examined in the as-polished state

(*) Murakami's Solution: 9.8 parts $K_3Fe(CN)_6$, 0.2 parts KOH, 90 parts H_2O.

(**) Acid Solution : Six parts HNO_3, 2 parts H 2 parts HF, 90 parts H_2O

flakes were then filtered off, washed thoroughly with methanol and warm heptane to remove the paraffins formed during the dissolution, and dried for 24 hrs at 105°C in a vacuum oven. The amount of graphite was then determined by combustion.

Approximately one-eighth of the experimental alloy material was analyzed for oxygen and nitrogen by the gas-fusion technique; low level impurities were, on a random sample selection basis, determined spectrographically in a semi-quantitative manner. No metal analyses were performed since the relative metal contents were not assumed to change to any significant extent during the experiments.

In general, it was found that the analyzed sample compositions, based on carbon, agreed to within one atomic percent with the weighed-in compositions. Oxygen contamination in all alloys analyzed was found to be below 120 ppm, and for the majority of the samples, even below 20 ppm; its possible effect upon the measured phase equilibrium data may therefore be disregarded.

Since the crystal structures of all phases were known from previous work, only powder patterns using Cu-K_α radiation were prepared. The film strips were measured on a Siemens-Kirem coincidence scale with micrometer (0.01 mm scale divisions) attachment. All exposures were evaluated with respect to nature and lattice dimensions of the phases present, and the X-ray data were correlated with the results gained by the other methods of investigation. The lattice parameter technique also was used to determine the compositions of the coexisting phases in the various two-phase fields, as well as to locate the vertices (boundary tie lines) of the three-phase equilibria occurring in the system.

IV. RESULTS

A. THE NIOBIUM-MOLYBDENUM BINARY SYSTEM

Melting point measurements on eight binary alloys showed a continuous increase of the solidus temperatures with the molybdenum concentration (Figure 5); the reproducibility of each measurement was better than ± 15°C, thus definitely ruling out the existence of a minimum melting point such as proposed by I.I. Kornilov and R.S. Polyakova(7). Our measurements of the lattice parameters of the metal solid solution agree closely with the values determined by H. Bückle(5) (Figure 6).

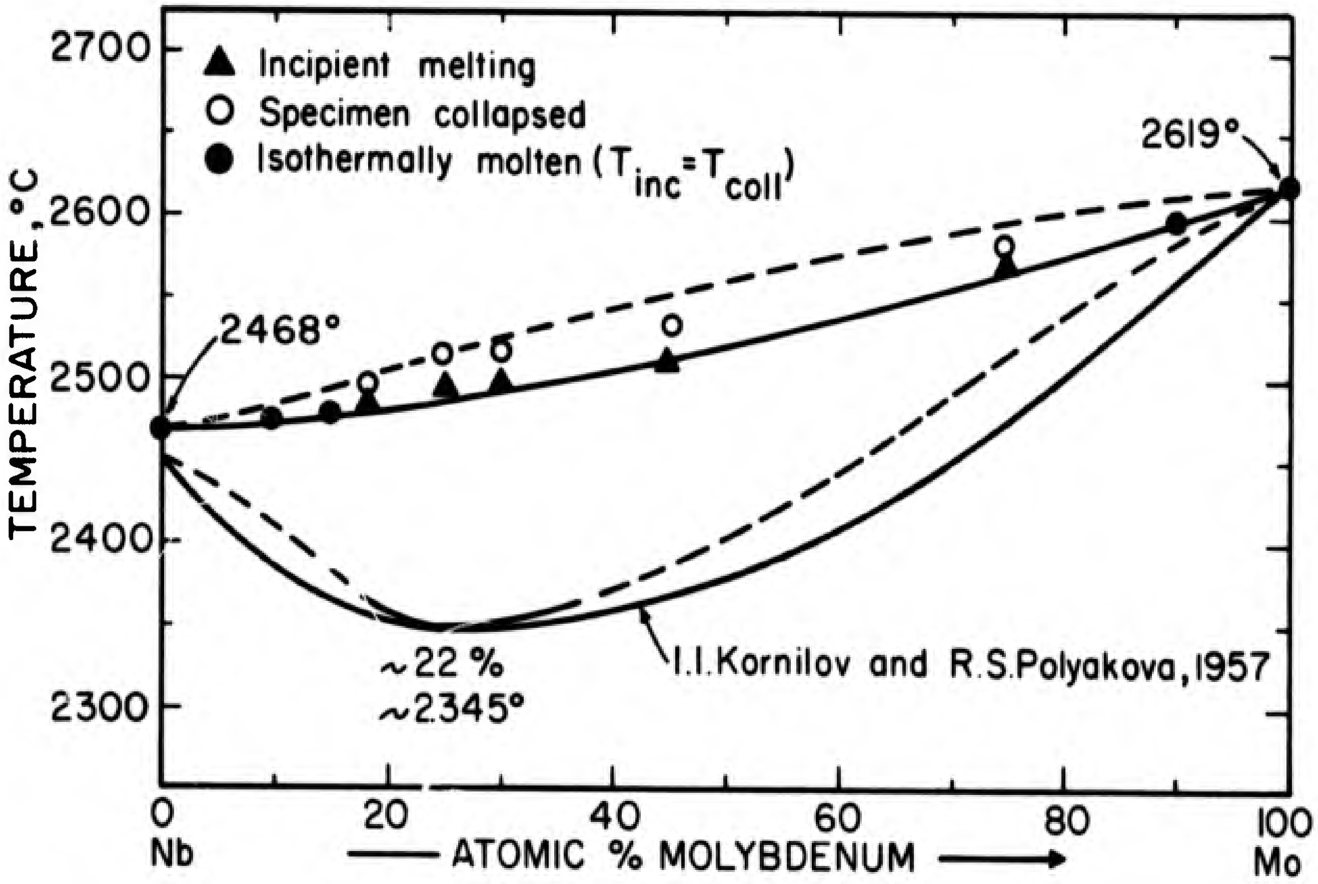

Figure 5. Melting Temperatures of Niobium-Molybdenum Alloys.

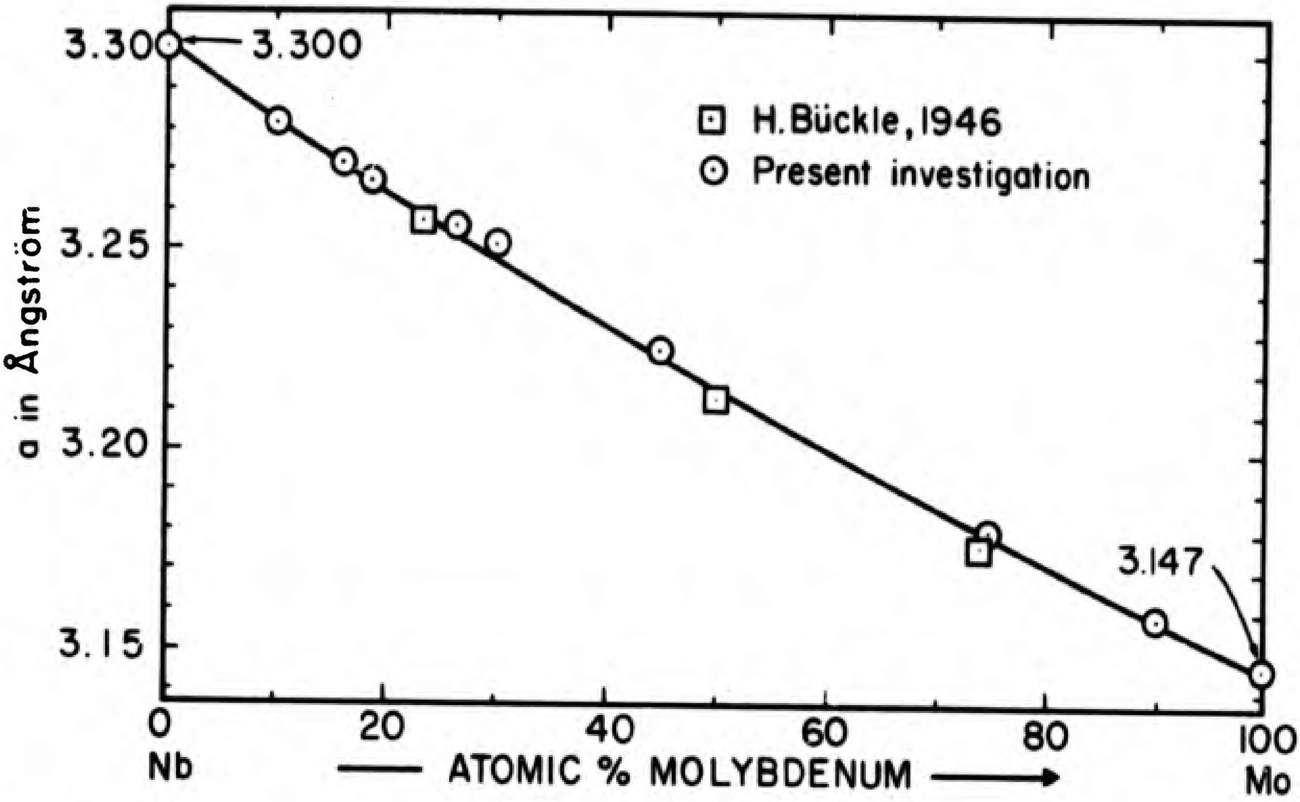

Figure 6. Lattice Parameters of the Niobium-Molybdenum Solid Solution

B. SOLID STATE EQUILIBRIA IN THE TERNARY Nb-Mo-C SYSTEM

The phase distribution in the temperature section at 1500°C (Figure 7) is very similar to the phase relations at 1900°C investigated earlier(2), although, as a result of the lower temperatures, the homogeneity ranges as well as the compositions of the coexisting phases assume slightly different values. The maximum molybdenum exchange in the niobium monocarbide at this temperature is 60 atomic percent; at this boundary, the carbon defect of the monocarbide phase is approximately 4 atomic percent. The lattice parameters of the carbide phases participating in the three-phase

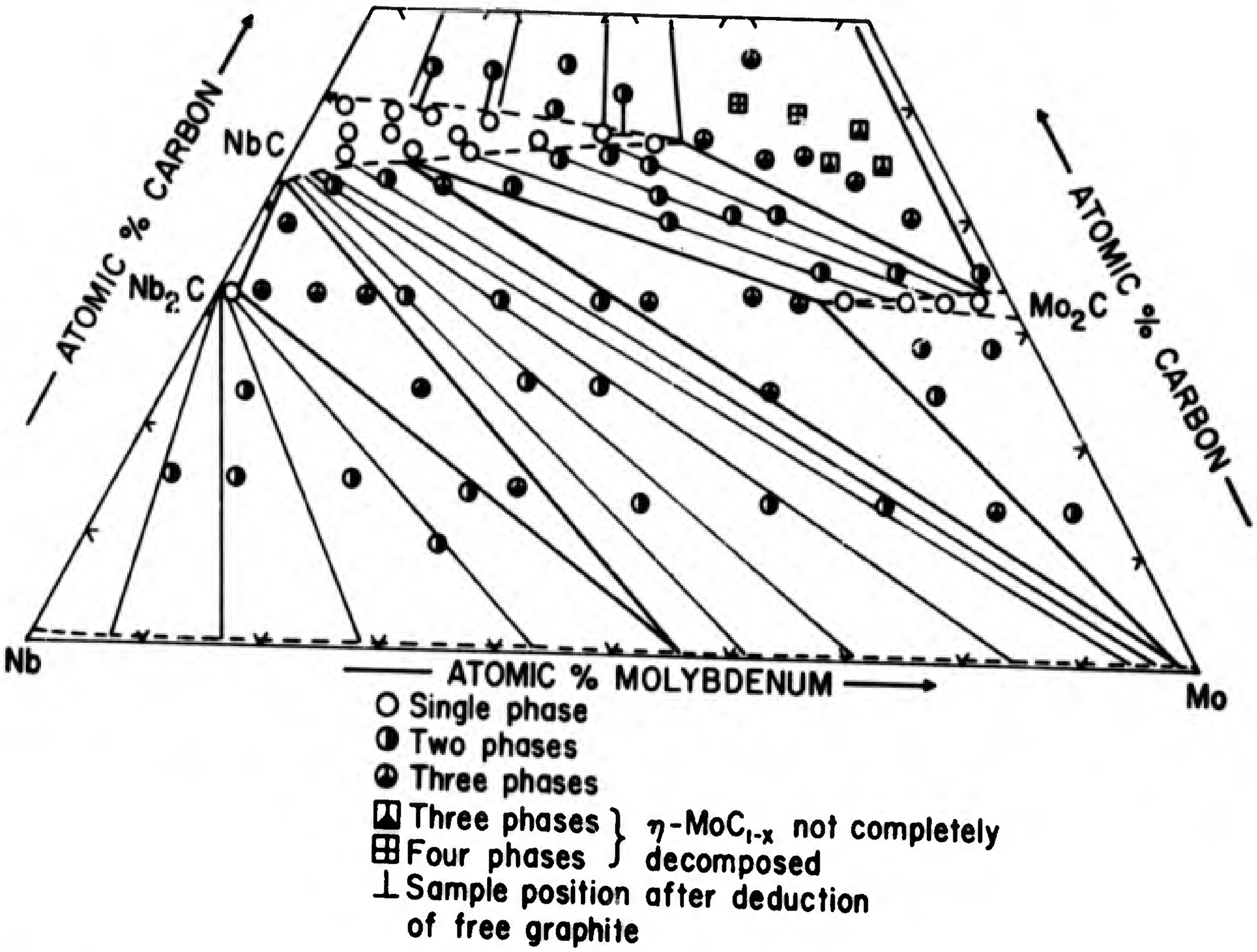

Figure 7. Qualitative X-Ray and Metallographic Phase Evaluation of the Alloys Equilibrated at 1500°C.

equilibrium: Monocarbide + Mo_2C-ss + graphite are respectively: a = 4.352 Å for the monocarbide, and a = 3.015 Å, c = 4.736 Å for the dimolybdenum carbide solid solution.

A further three-phase equilibrium, $(Nb,Mo)C_{1-x}$-ss + Mo_2C-ss + (Nb,Mo)-ss terminates the dimolybdenum carbide phase towards the ternary phase field. The niobium exchange in Mo_2C at this equilibrium temperature is approximately 25 atomic percent (a = 3.020 Å, c = 4.764 Å). This subcarbide composition is in equilibrium with a metal alloy containing approximately 2 atomic percent niobium (a = 3.150 Å); the vertex of the defect monocarbide solid solution lies at a molybdenum exchange of 17 atomic percent and a carbon content of 44 atomic percent.

Di-niobium carbide dissolves less than three mole percent Mo_2C at this temperature (a = 3.125 Å, c = 4.965 Å for Nb_2C; a = 3.115 Å, c = 4.944 Å for the composition at the three-phase boundary). The other vertices of the three-phase equilibrium: Nb_2C-ss + monocarbide + metal solution are located at 1 atomic percent molybdenum exchange in the monocarbide, and at 55 atomic percent molybdenum (a = 3.21 Å) in the metal-solution. The course of the tie lines within the two-phase fields: Mo_2C-ss + $(Nb, Mo)C_{1-x}$-ss; (Nb, Mo)-ss + Mo_2C-ss; (Nb, Mo)-ss + $(Nb,Mo)C_{1-x}$-ss; and (Nb, Mo)-ss + Nb_2C-ss, as determined by lattice parameter measurements, shows a pronounced enrichment of niobium in the carbide phases. This finding indicates that the niobium carbides have comparatively higher stability than the binary molybdenum-carbon phases. Quantitative relationships concerning the partition equilibria in the system will be developed and discussed in a later section.

Basically, the same phase distribution was obtained for 1900°C, although the solid solubilities in the subcarbide phases are somewhat larger, and the equilibria near the binary molybdenum-carbon system are modified by the appearance of the η-phase. The maximum solubilities in the various intermediate phases are approximately; 83 mole% MoC_{1-x} in niobium monocarbide (Figure 8); 29 mole% Nb_2C in Mo_2C (a = 3.021 Å, c = 4.778 Å, based on indexing according to the L'3 type); 4 mole% Mo_2C in Nb_2C (a = 3.110 Å, c = 4.933 Å); and an exchange of 4 atomic percent niobium in -MoC_{1-x} (a = 3.017 Å, c = 4.66 Å).

The results of the system section studies at 2200°C are of special interest since this temperature lies near the solidus temperatures of excess metal-containing ternary alloys, and the measured terminal compositions of the solid phases should, therefore, closely represent the compositions entering into liquidus reactions.

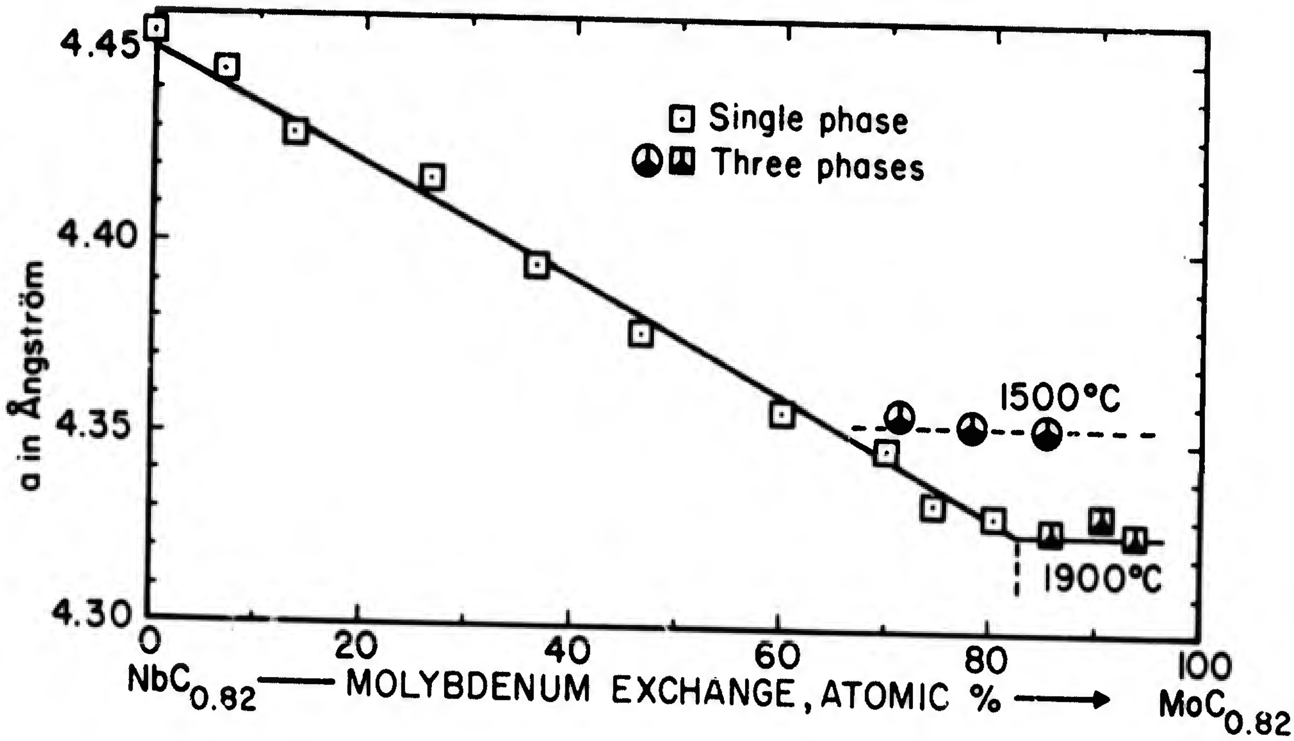

Figure 8. Lattice Parameters of the Cubic Monocarbide Solution Along the Section $NbC_{0.82}$-$MoC_{0.82}$, and Phase Boundary Values at 1500°C and 1900°C.

From the phase evaluation of the alloys homogenized at 2200°C (Figure 9), it can be seen that the cubic phases form a continuous series of solid solutions; the lattice parameters show a slight positive deviation from a linear relationship (Figure 10). Compared to the binary α-MoC_{1-x} phase where tin-quenching is required, the decomposition of the ternary solid solution occurs slowly, even at small niobium concentrations. As an example, for compositions containing more than 5 mole percent niobium carbide, cooling rates of approximately 15°C per second are sufficient to retain the cubic monocarbide solution; fairly long annealing times at lower temperatures (< 1600°C) are necessary to decompose solid solutions containing less than 80 mole% MoC_{1-x}.

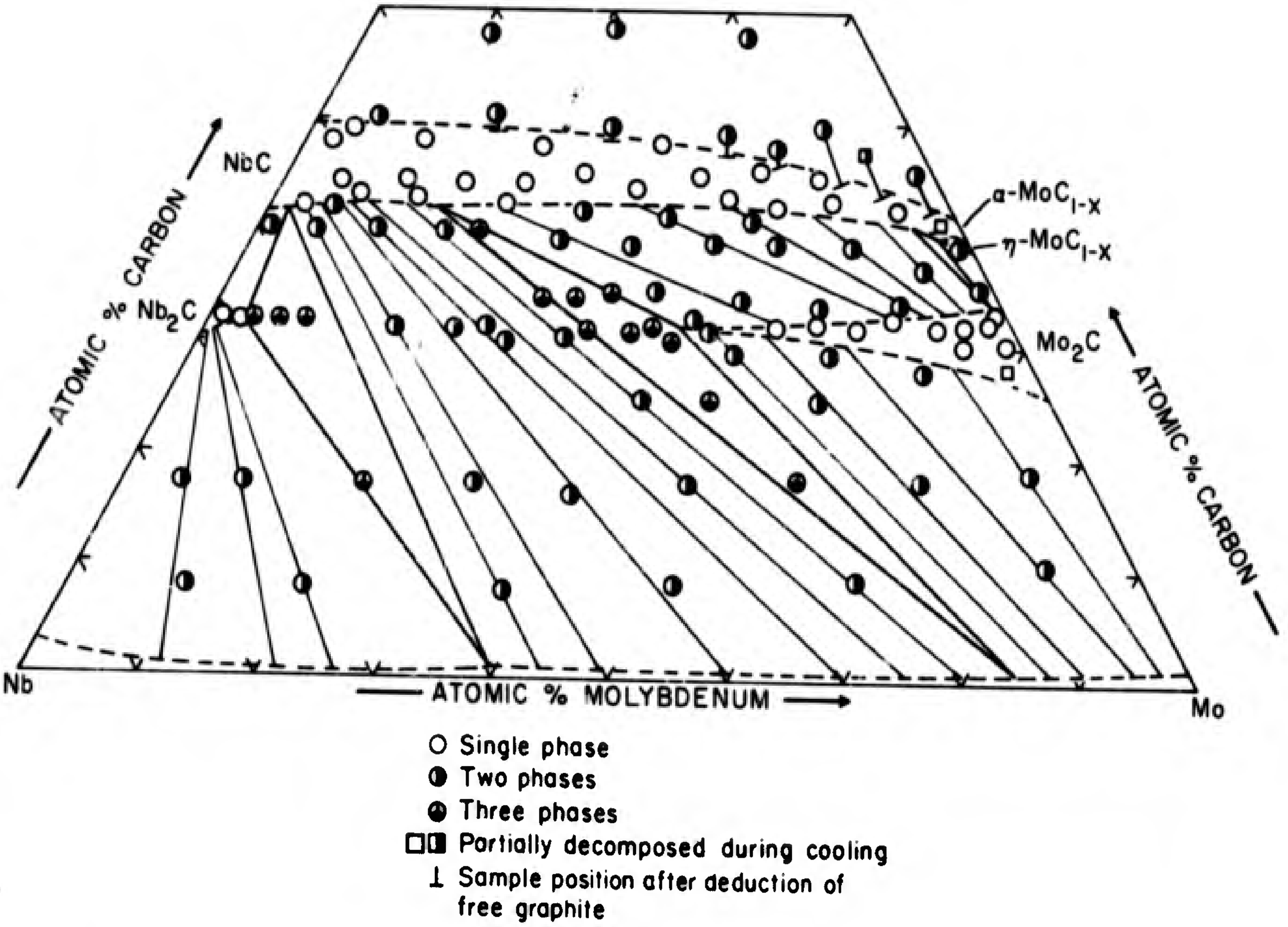

Figure 9. Qualitative X-Ray and Metallographic Phase Evaluation of the Alloy Series Equilibrated at 2200°C.

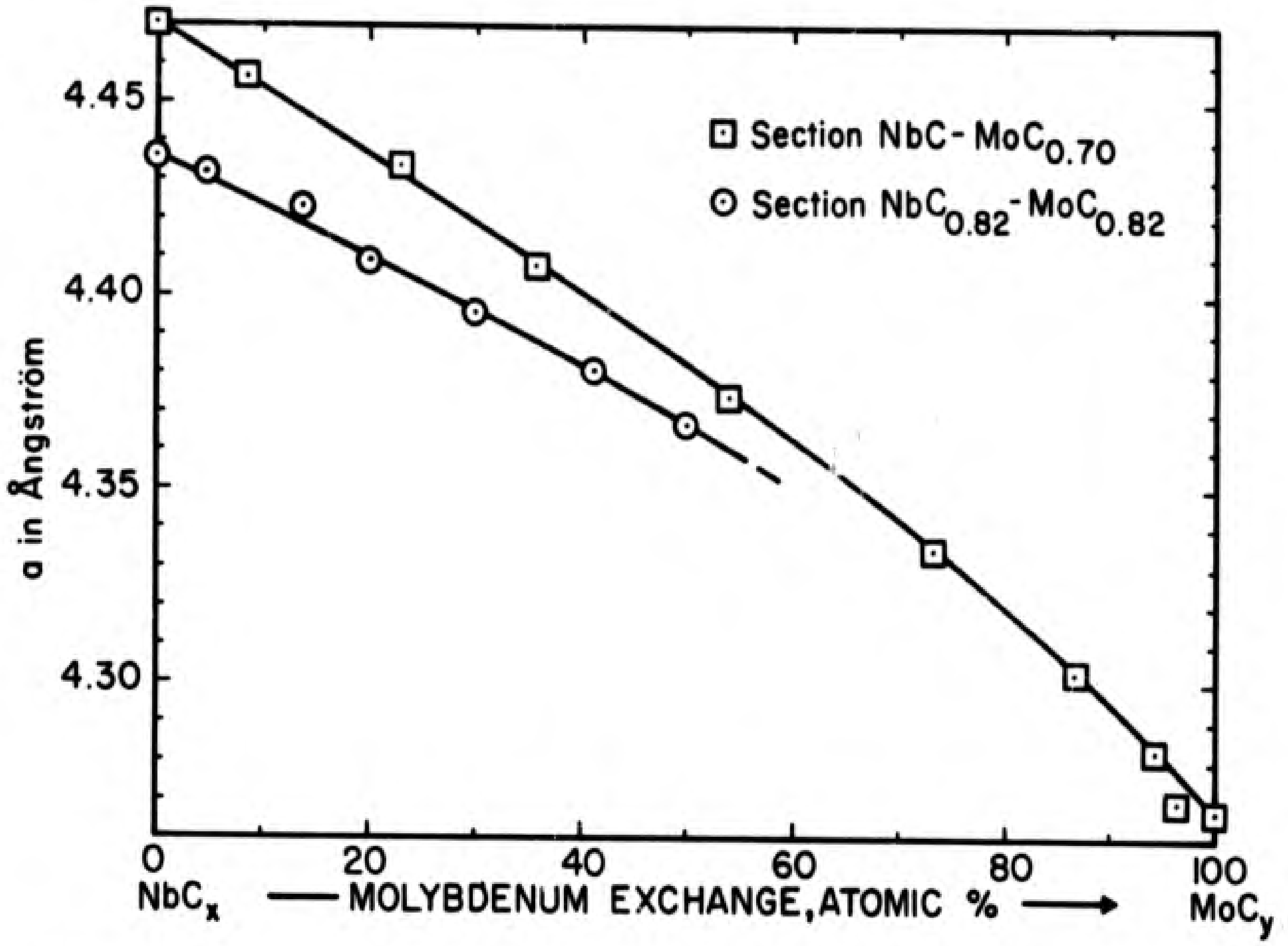

Figure 10. Lattice Parameters of Monocarbide Alloys. (Alloys Rapidly Cooled from 2200°C).

Dimolybdenum carbide dissolves approximately 44 mole % Nb_2C at this temperature (Figure 11), whereas the solid solubility of Mo_2C in Nb_2C is less than 5 mole percent. X-ray data indicated that the appearance of the η-phase is restricted to a very narrow composition range near the molybdenum-carbon binary system.

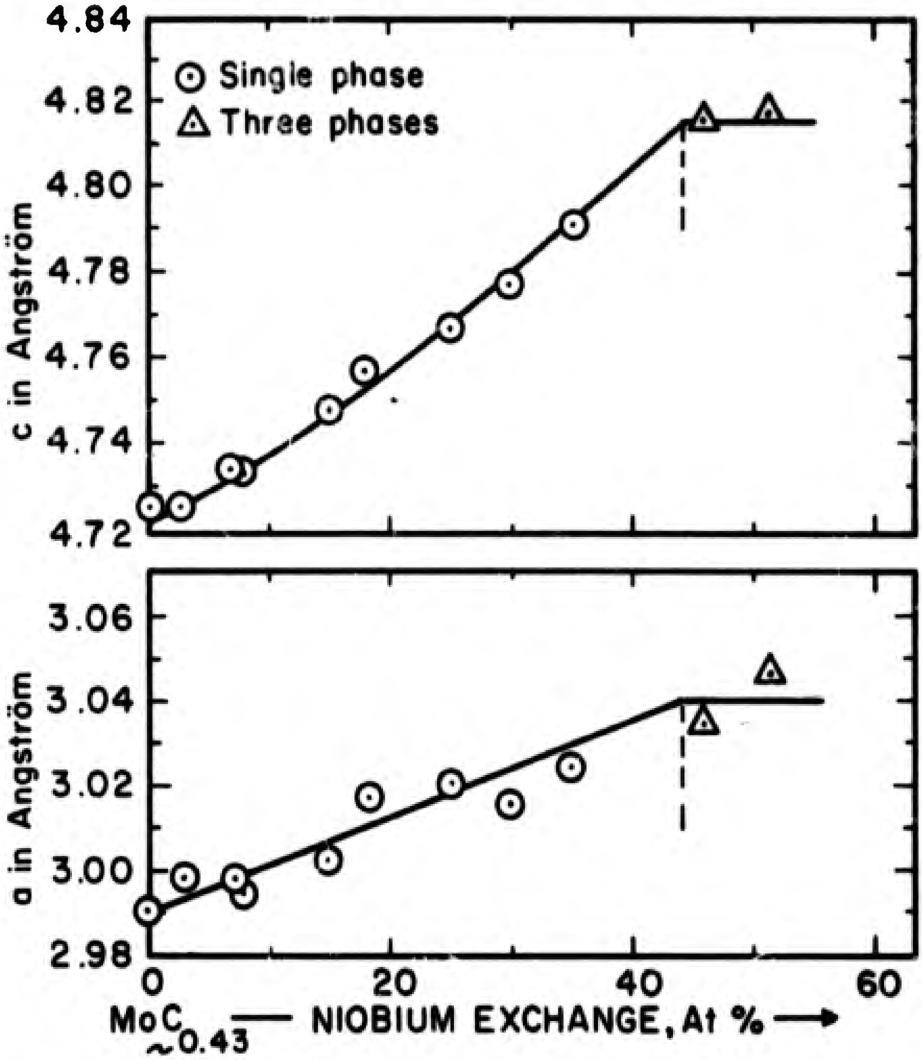

Figure 11. Lattice Parameters of the Mo_2C Solid Solution. (Alloys Rapidly Cooled from 2200°C. Parameters are Based on Indexing According to the L'3-type).

C. PHASE EQUILIBRIA AT HIGH TEMPERATURES

From the Nb + Nb_2C eutectic isotherm at 2353°C, the solidus temperatures of ternary alloys in the composition range Me + Me_2C are lowered only slightly by molybdenum substitutions up to 50 atomic percent (Figure 12); beyond this range, the solidus temperatures drop rapidly to the binary Mo + Mo_2C eutectic isotherm at 2200°C. All alloys located at, or or close to, the eutectic trough melted fairly isothermally, suggesting that

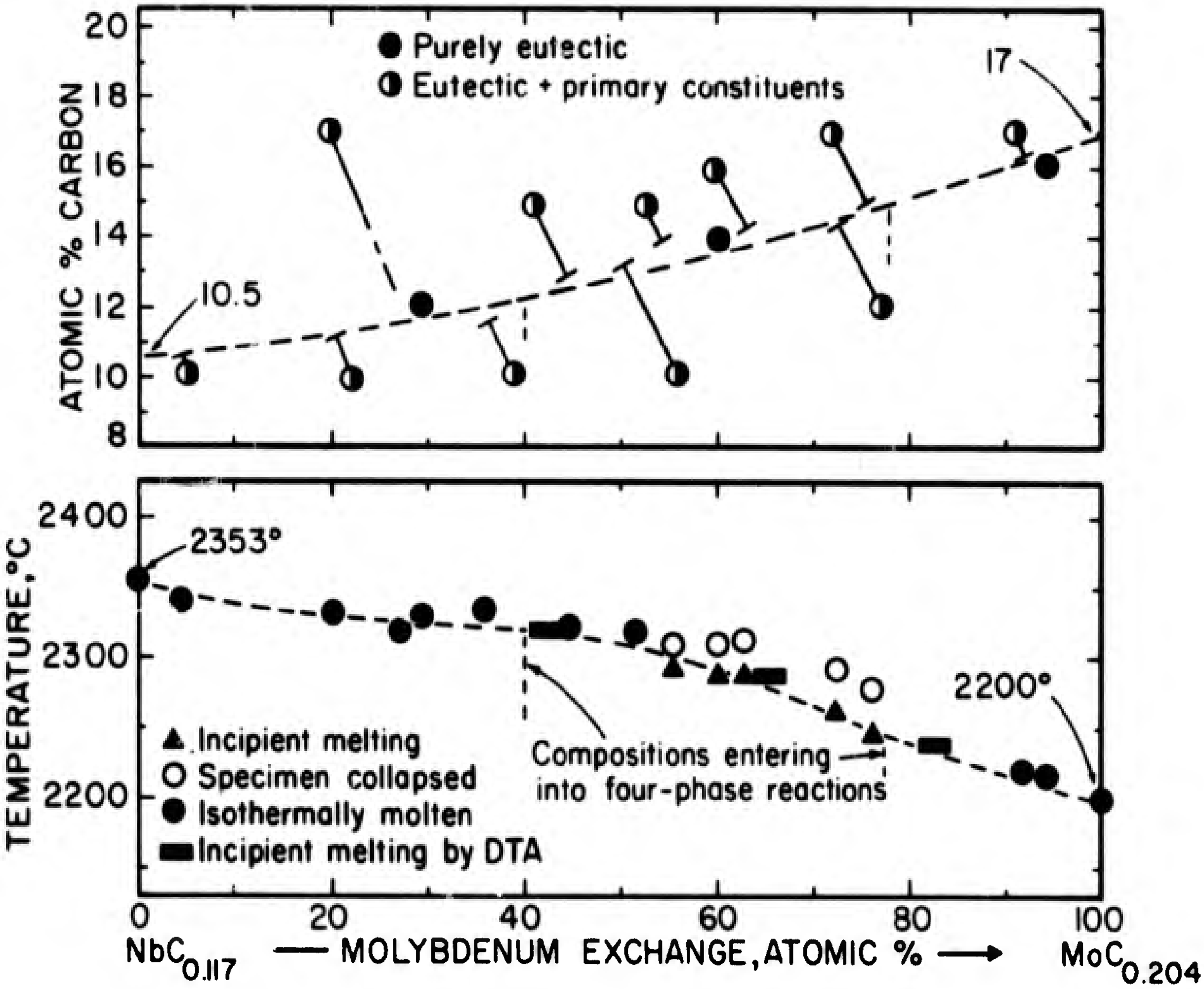

Figure 12. Temperatures (Bottom) and Location (Top) of the Metal-Rich Eutectic Trough in the Nb-Mo-C System.

only a small temperature gap exists between solidus and liquidus. This behavior is also reflected in the microstructures, which closely resemble the structures found for binary eutectics. The eutectic structure formed in the ternary changes from a metal-matrix type, found in the binary niobium-carbon system, gradually to a carbide matrix type with exchange of niobium by molybdenum (Figures 13, 14, and 15).

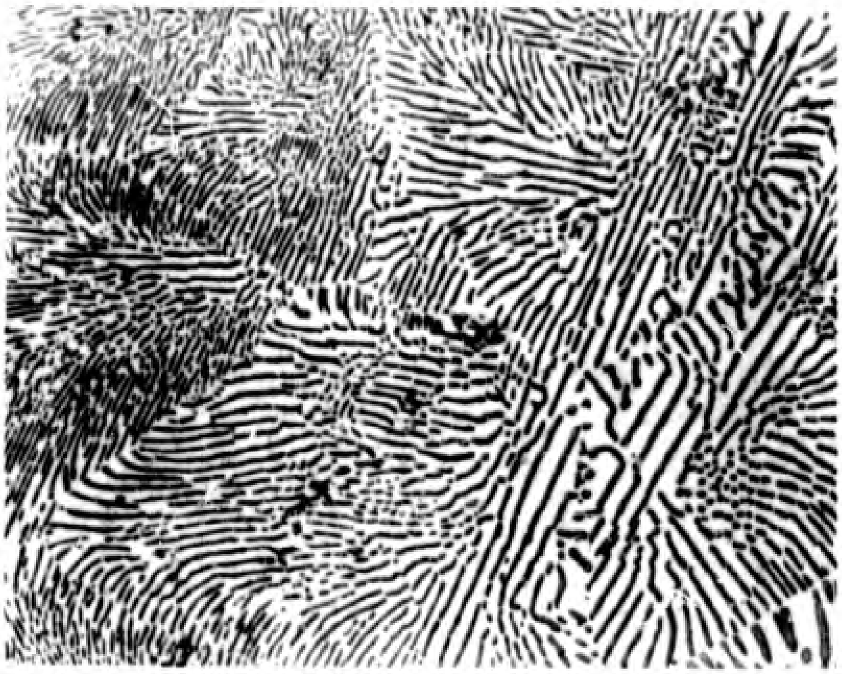

Figure 13. Nb-Mo-C (85-5-10 At.%), Rapidly Cooled from 2350°C. X750

Eutectic-like Solidification Structure Near the Niobium-Carbon Binary.

Matrix : (Nb, Mo)-ss

Discontinuous Phase: Nb_2C-ss

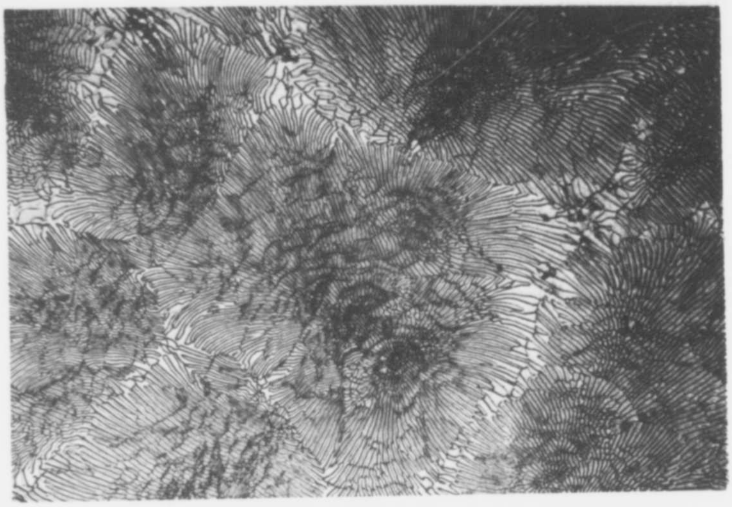

Figure 14. Nb-Mo-C (26-60-14 At.%), Rapidly Cooled from 2280°C. X560

Lamellar Eutectic-Type Structure Consisting of (Nb, Mo)-ss and $(Nb, Mo)_{1-x}$-ss.

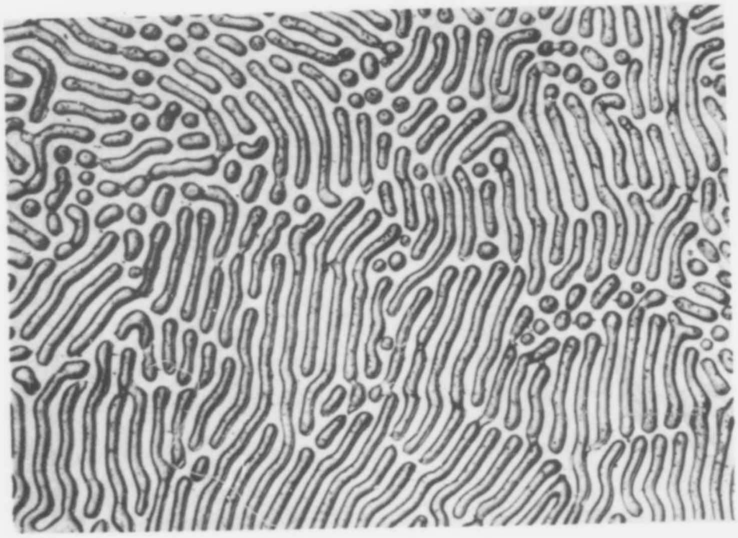

Figure 15. Mo-C (17 At.% C), Cooled at 14°C per Second from 2220°C. X375

Mo + Mo_2C Eutectic.

Matrix : Mo_2C

Discontinuous Phase: Mo

It should be noted, however, that the phase constituents participating in the bivariant eutectic solidification vary with the relative metal content: Up to approximately 30 atomic percent molybdenum, the metal solution is in equilibrium with the niobium subcarbide phase; in the range from 35 to 70 At.% Mo, the metal phase coexists with the monocarbide, and from 80 to 100 At.% Mo, the metal phase is in equilibrium with the dimolybdenum carbide and solid solution. The cross-over between these various ranges is marked by four-phase reactions, which replace the equilibria subcarbide + metal-phase by equilibria formed between the monocarbide and melt. These four-phase reactions were delineated in detail by measurements of the solidus temperatures as well as by metallographic and X-ray studies mainly on an alloy series positioned across the section Nb_2C-Mo_2C (Figures 16 and 17): An alloy Nb-Mo-C (64-3-33 At.%) proved to be single-phased after quenching from 2300 and 2400°C, but the alloy containing 8 mole percent molybdenum showed monocarbide and metal phase as the major constituents following rapid cooling of the specimen from 2650°C. Smaller quantities of subcarbide present in the alloy apparently had formed by interaction between melt and monocarbide at temperatures below the four-phase isotherm, resulting in a peritectic-like non-equilibrium structure (Figure 18). The X-ray pattern of the alloy containing 12 mole percent molybdenum, after quenching from 2600°C, showed only monocarbide and metal phase; the micrograph of this alloy (Figure 19) reveals primary crystallized monocarbide, with typically localized precipitations, in a metal + monocarbide eutectic matrix.

Similar microstructures (Figure 20) were observed at the four-phase plane near the terminal solid solution of Mo_2C, i.e. upon rapid cooling, non-equilibrium mixtures consisting of metal-phase, unconverted monocarbide, and dimolybdenum carbide solid solution are formed by interaction between liquid and monocarbide according to the reaction scheme:

$$L + (Nb,Mo)C_{1-x}\text{-ss} \rightarrow (Mo_2C)\text{-ss} + (Nb,Mo)\text{-ss}$$

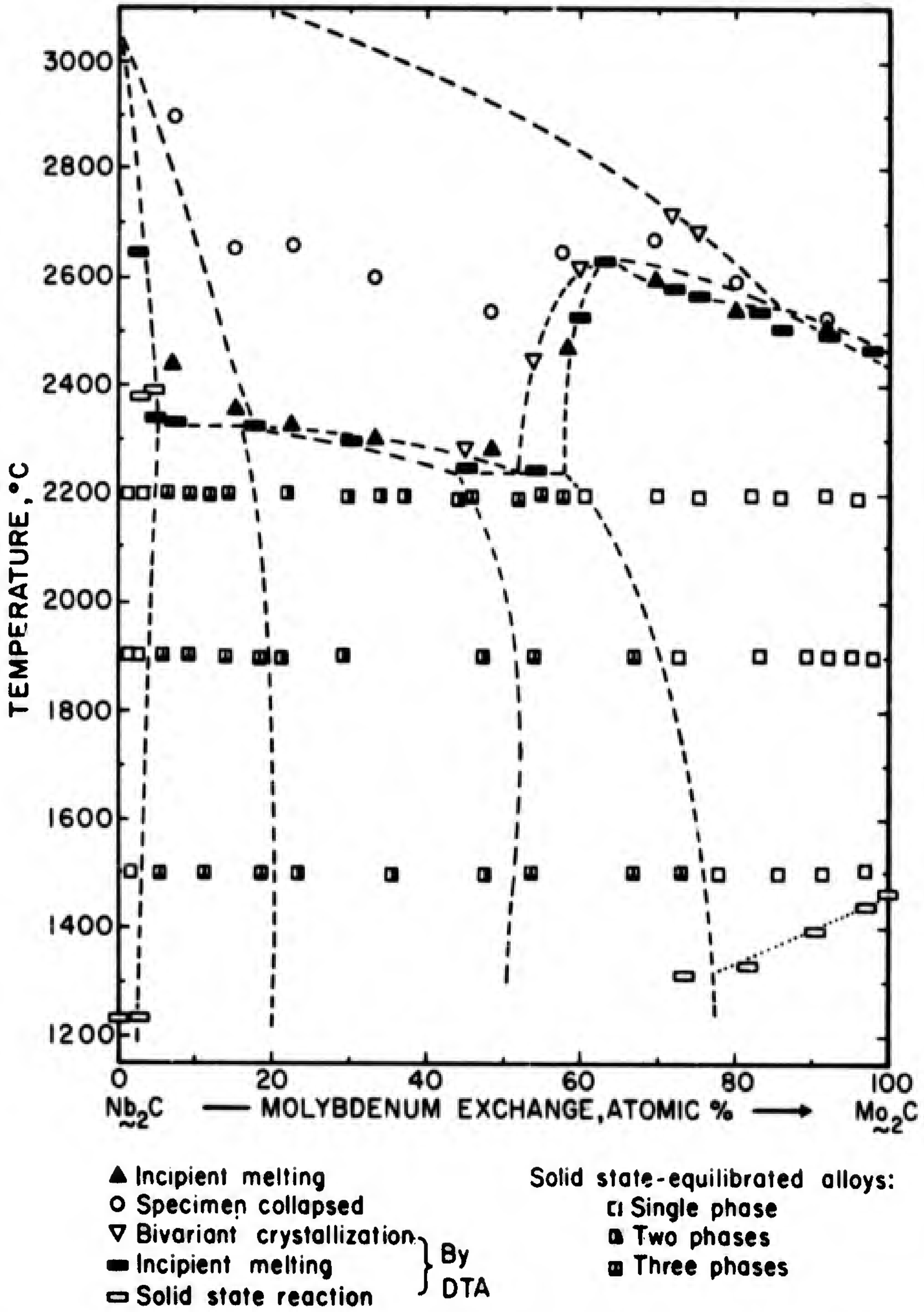

Figure 16. Melting and Qualitative Phase Evaluation of Alloys Located on the Nb_2C-Mo_2C Section.

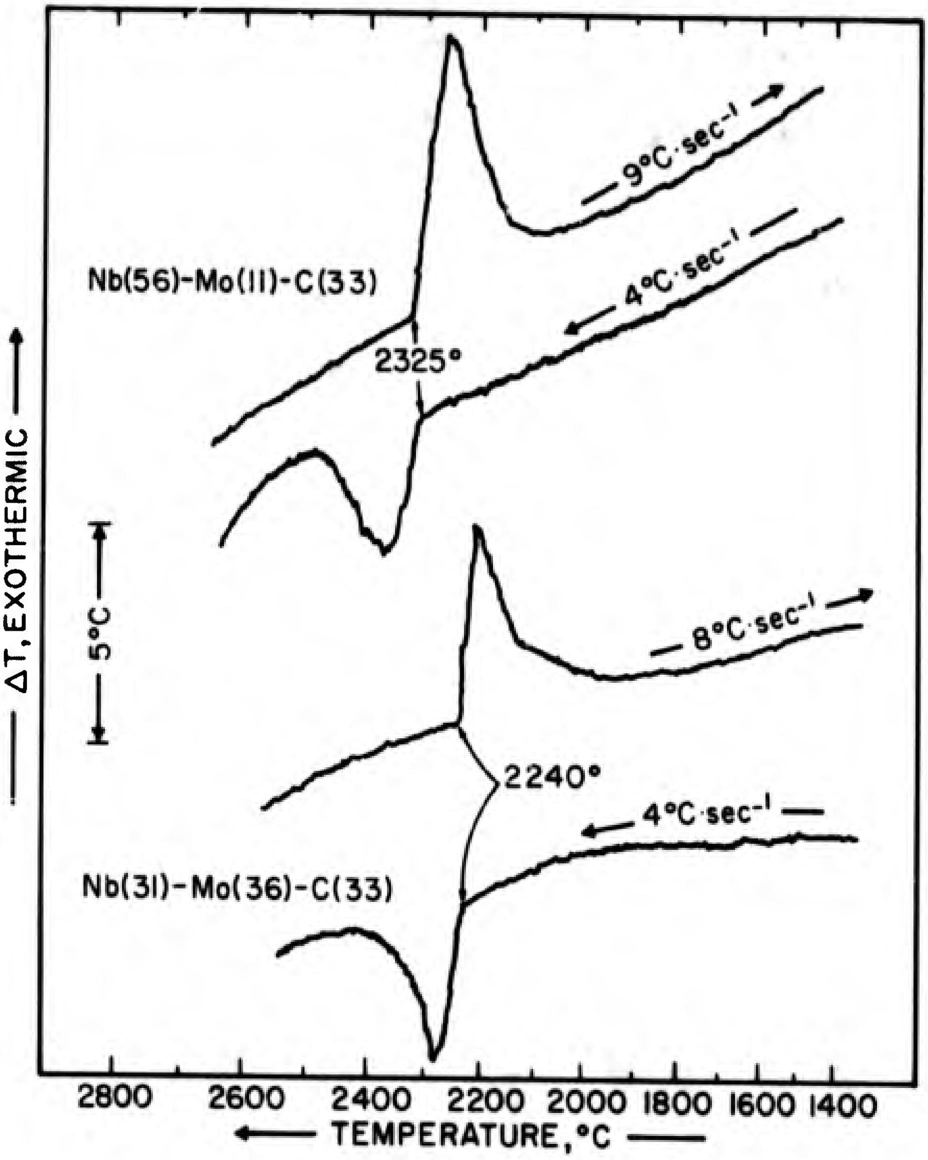

Figure 17. DTA-Thermograms of Two Ternary Alloys Participating in Four-Phase Reactions.

(Concentrations in Atomic Percent)

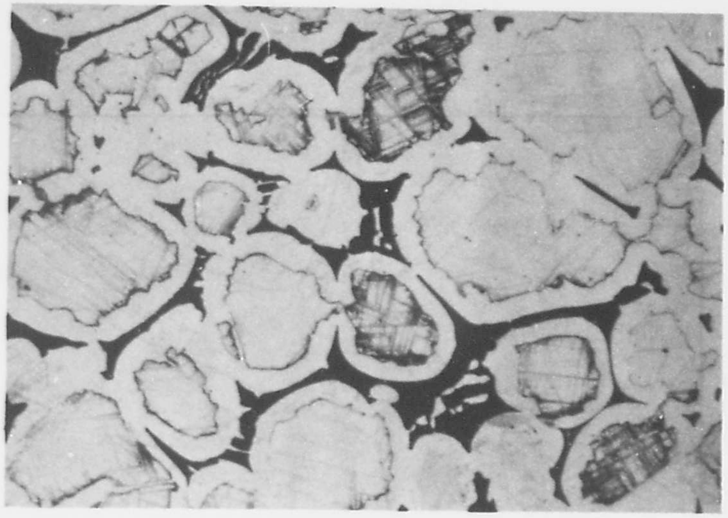

Figure 18. Nb-Mo-C (59-8-33 At.%), Cooled at Approximately 50°C per Second from 2650°C. X600

Peritectic-Type Non-equilibrium Mixture Resulting from the Four-Phase Reaction:

L + (Nb, Mo)C$_{1-x}$-ss — (Nb, Mo)$_2$C-ss + (Nb, Mo)-ss

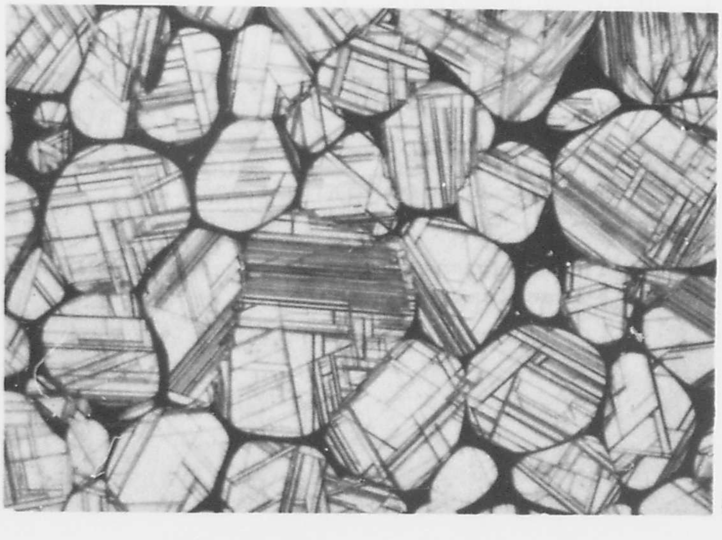

Figure 19. Nb-Mo-C (56-12-32 At.%), Rapidly Cooled from 2600°C. X600

Primary Monocarbide with Intragranular, Localized Metal Precipitations, Contained in a Matrix of Metal + Monocarbide Eutectic.

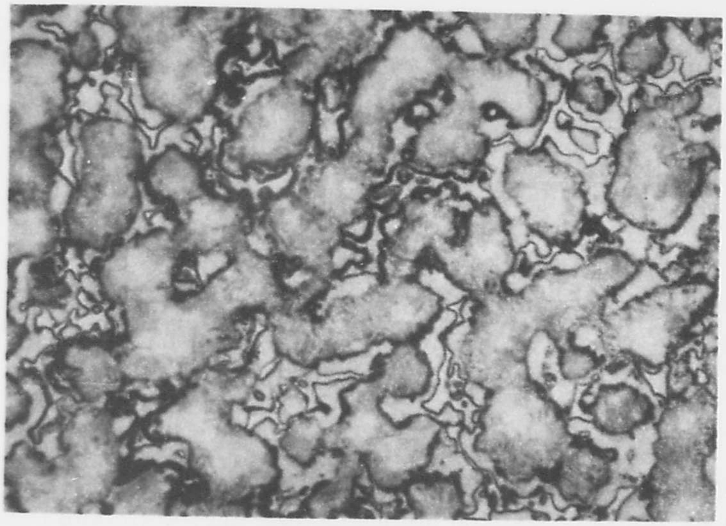

Figure 20. Nb-Mo-C (31-36-33 At.%), Cooled at Approximately 10°C per Second from 2700°C. X560

Non-equilibrium Reaction Mixture, Consisting of (Nb, Mo)C_{1-x}-ss (Primary Constituent), Mo_2C-ss, and (Nb, Mo)-ss.

From 2240°C, the temperature of the four-phase plane, the solidus temperatures for the dimolybdenum carbide solid solution increase within a small concentration range to a maximum at 2640°C and approximately 64 mole percent Mo_2C (Figure 16). Melting at this composition, however, occurs under disproportionation, as evidenced by the observation that the specimens, when quenched from above solidus, contained a non-equilibrium mixture of monocarbide, subcarbide, and metal phases. At higher molybdenum contents, the solidus temperatures of the subcarbide solution are lowered, and as the boundary system is approached, melting changes from a peritectic to a maximum type; the transition point lies at approximately 87 mole percent Mo_2C.

Concerning the type of reaction involved in the ternary decomposition (melting) of the dimolybdenum carbide solid solution at the maximum solidus point, among the two types of processes to be considered, melting according to a class III peritectic-reaction can be ruled out, since this would require a particular monocarbide composition to coexist with two different melts at the four-phase temperature plane, i.e. it would require a very anomalous mixing behavior of the melt. Instead, the experimental evidence suggests that the two, three-phase equilibria

$$L\ (1) + Mo_2C\text{-ss}\ (1) + (Nb, Mo)C_{1-x}\ (1)$$

and

$$L\ (2) + Mo_2C\text{-ss}\ (2) + (Nb, Mo)C_{1-x}\ (2)$$

of which the first results from the four-phase reaction at 2240°C, and the second originates at the transition point between peritectic and maximum-type melting of the subcarbide, merge into a limiting tie line.

The maximum solidus temperatures of the monocarbide solution increase gradually from 2600°C, the melting point of α-MoC_{1-x}, to 2613°C, the congruent melting point of niobium monocarbide. It should be noted that the datum points shown in Figure 21 were selected from over 30 melting point measurements covering the entire solidus envelope of the monocarbide solid solution. To either side of the concentration line of the maximum solidus the melting temperatures drop rapidly to lower values. Due to the comparatively large melting point differences of the boundary phases, the differences between the liquidus and solidus temperatures, and consequently the concentration differences between the coexisting phases, become rather large. As a result, alloys quenched from liquidus temperatures were heavily cored (Figure 22), and the X-ray patterns were very diffuse; as a rule, only the low-angle edges of the diffraction maxima (corresponding to the initially crystallizing, niobium-richer compositions) were sharp, whereas the higher angle end of these maxima, corresponding to molybdenum-richer

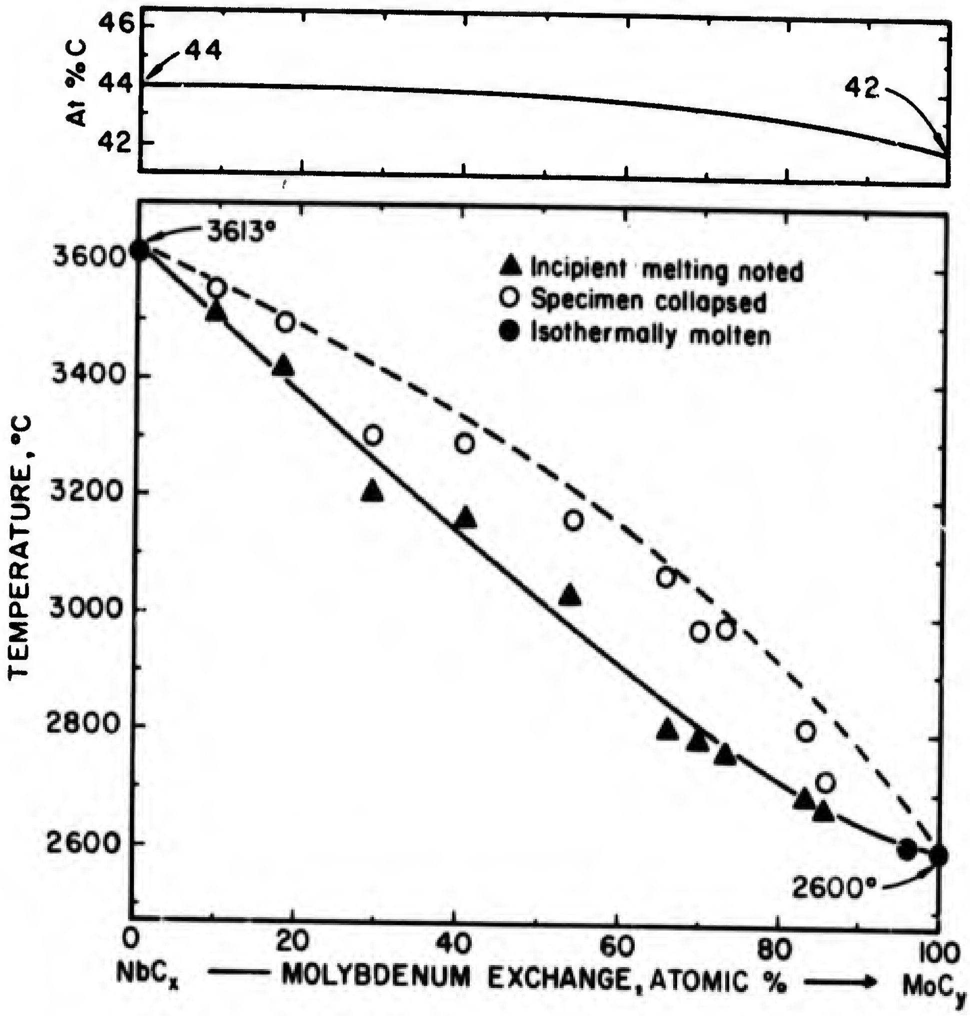

Figure 21. Maximum Solidus Temperatures of the Cubic Monocarbide Phase. Top: Concentration Line of the Maximum Solidus.

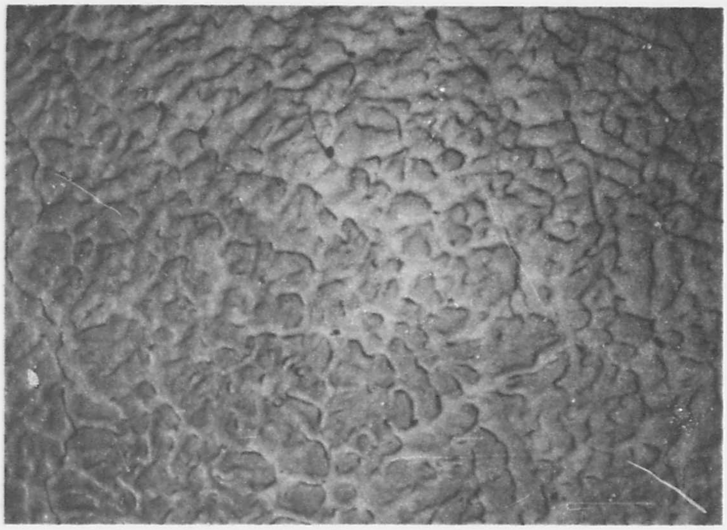

Figure 22. Nb-Mo-C (28-25-47 At.%), Quenched from 3260°C. X375
Cored Monocarbide Solution

compositions, gradually merged with the film background. Although the analysis of these patterns yielded some information regarding the compositions of the phases coexisting in the liquidus + solidus region, for the purpose of lattice parameter measurements, duplicate samples were, after melting, re-equilibrated at slightly subsolidus temperatures and then quenched. Metallographic analysis showed the microstructure of these alloys to be homogeneous (Figure 23), and the X-ray patterns also were sharp.

DTA cooling runs on two alloys having compositions of Nb-Mo-C (2-56-43 At.%) and (6-51-43 At.%) showed incipient (solid state) decomposition temperatures of 1940°C and 1930°C, respectively, for the monocarbide solution. These temperatures are only slightly lower than the eutectic isotherm of the binary α-MoC_{1-x} phase. In these samples, a second,

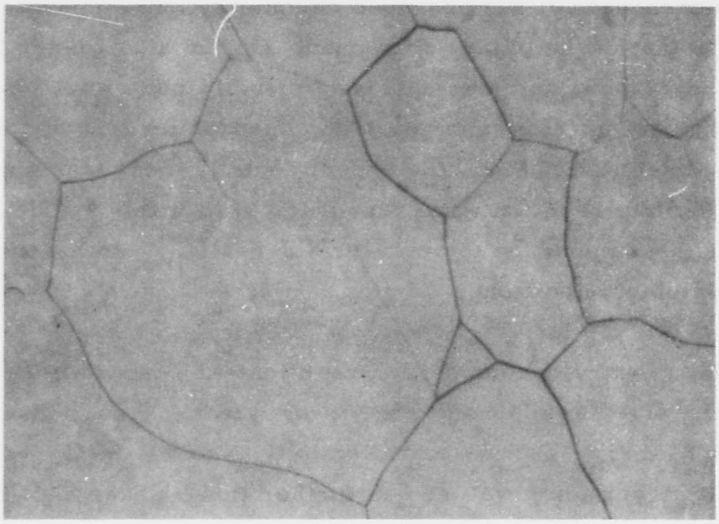

Figure 23. Nb-Mo-C (40-18-42 At.%), Melted at 3250°C, X600
Reequilibrated for 15 Minutes at 3000°C and Quenched.
Single Phased, Homogeneous Monocarbide.

solid state reaction in the vicinity of 1600°C was attributed to the decomposition of the η-MoC$_{1-x}$-phase, formed as a reaction product in the disproportionation of the monocarbide. This finding was confirmed by X-ray analysis of quenched alloys. In two further alloys, which contained 2 and 3 mole percent niobium, but had a carbon content of 36 atomic percent, only the thermal arrest due to the decomposition of the η-MoC$_{1-x}$ phase was detected. The measured decomposition temperatures, however, were approximately 100°C lower than that of the binary phase.

From the phase distribution determined at lower temperatures, combined with the results of the quenching and DTA-studies, the higher decomposition temperatures in the carbon-richer alloys will have to be attributed to the fact that the limiting tie line of the equilibrium:

$(Nb, Mo)C_{1-x}$-ss + η-MoC_{1-x}-ss + C terminates very near the molybdenum carbon binary; consequently, the observed decomposition temperatures correspond closely to that of the binary compound. On the other hand, in alloys which are lower in carbon, and thus consist either of single phase η-MoC_{1-x}, or contain in addition, Mo_2C and monocarbide, only the ternary decomposition of the η-phase is detectable. Since the experimentally measured temperatures for the solid state reaction were reproducible to within ± 25°C, it was concluded that the decomposition temperature of η-MoC_{1-x} is lowered to 1550°C by small niobium additions.

The ternary decomposition reaction can be readily reconstructed by considering that in addition to the two, three-phase equilibria: $(Nb, Mo)C_{1-x}$-ss + η-MoC_{1-x}-ss + C, and $(Nb,Mo)C_{1-x}$-ss + η-MoC_{1-x}-ss + Mo_2C-ss, which originate at higher temperatures, a further three-phase equilibrium Mo_2C-ss + η-MoC_{1-x}-ss + C, is introduced by the binary decomposition of η-MoC_{1-x} at 1655°C. These three equilibria combine at 1550°C in a class I (eutectoid) four-phase reaction according to

$$\eta\text{-MoC}_{1-x}\text{-ss} \xrightarrow{T \leq 1550^\circ C} \text{Mo}_2\text{C-ss} + (\text{Nb, Mo})\text{C}_{1-x}\text{-ss} + \text{C}$$

In the composition area monocarbide + graphite, the curve connecting the measured solidus-temperatures along the eutectic trough shows a slight inflection around 50 atomic percent metal exchange. Considering the large differences of the binary eutectic temperatures, one observes that the gap between the solidus and the liquidus (dashed line in Figure 24), is surprisingly small. Nevertheless, as a result of the bivariant solidification, eutectic-like structures were obtained only in alloys located near the respective binaries, such as shown in Figure 25. A typical microstructure for the bivariantly solidified eutectic is shown in Figure 26.

With increasing niobium content and temperature, the maximum bound carbon content of the monocarbide solution increases; as an

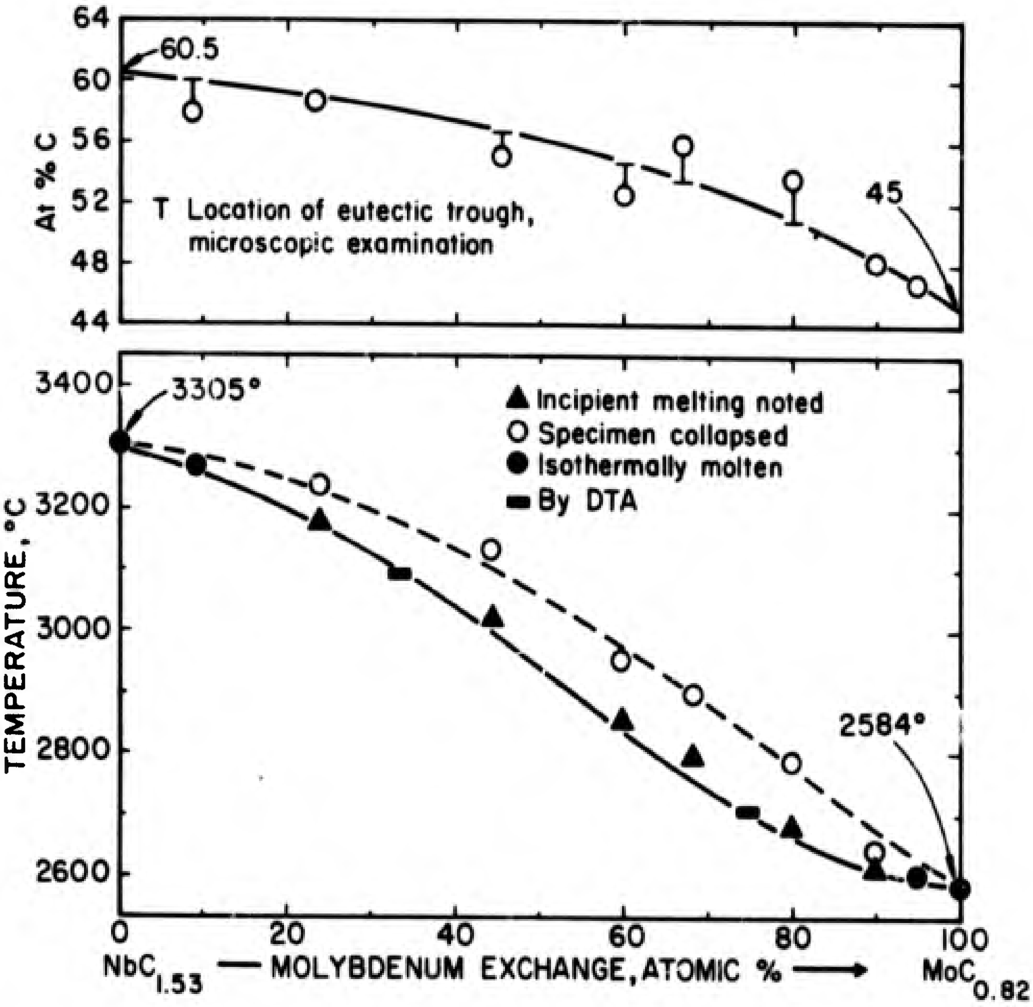

Figure 24. Experimental Solidus Temperatures (Bottom) and Location of the Eutectic Trough (Top) Between the Monocarbide Solution and Graphite.

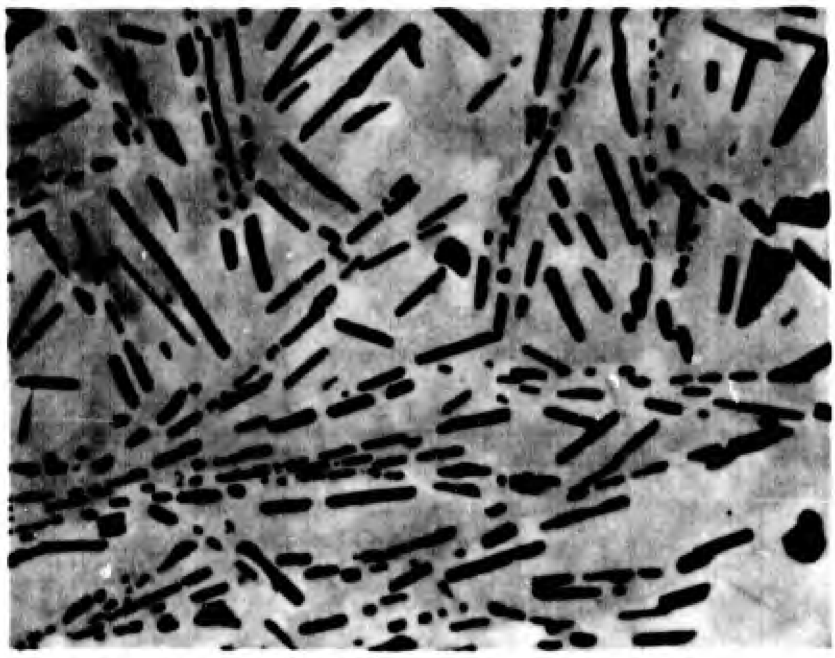

Figure 25. Nb-Mo-C (34-10-56 At.%), Cooled at Approximately 100°C per Second from 3250°C. X600

Eutectic-like, (Nb,Mo)C$_{1-x}$-ss + C, Solidification Structure in an Alloy Located Near the Niobium-Carbon Boundary System.

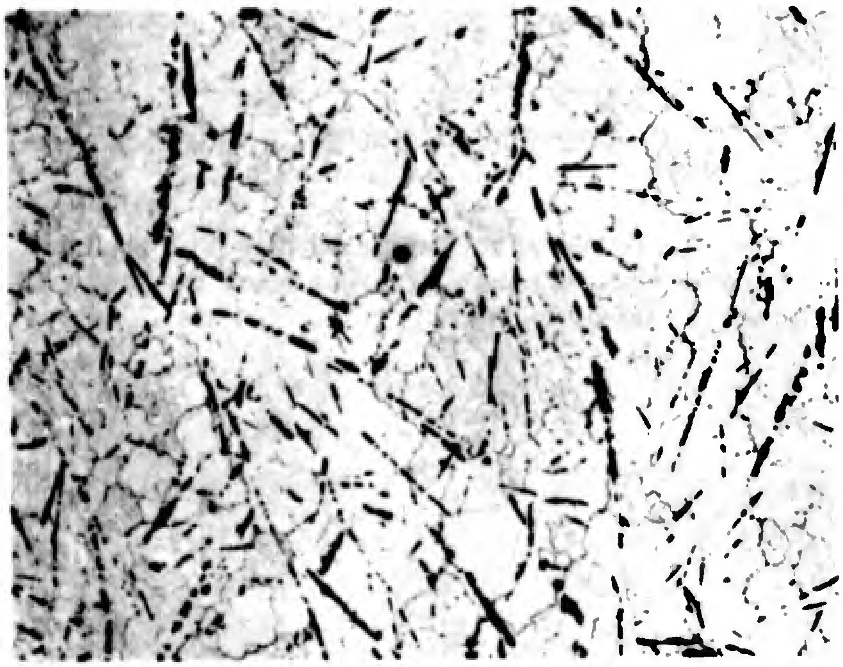

Figure 26. Nb-Mo-C (20-30-50 At.%), Cooled at Approximately 100°C per Second from 3000°C. X100

Typical Microstructure, Consisting of Monocarbide and Graphite, Formed by Bivariant Solidification on the Eutectic Trough.

example, at an metal exchange of 50 atomic percent and a temperature of 2500°C, the carbon-rich boundary was located between 48 and 58.5 At.% C; whereas, at the same temperature, the boundary of the binary molybdenum carbide lies at approximately 42.5 At.% C. An alloy, Nb-Mo-C (3-52-45 At.%), showed only traces of graphite at the grain boundaries following quenching from 2500°C (Figure 27), whereas another alloy, having the same relative metal content, but only 44 atomic percent carbon, was single phased.

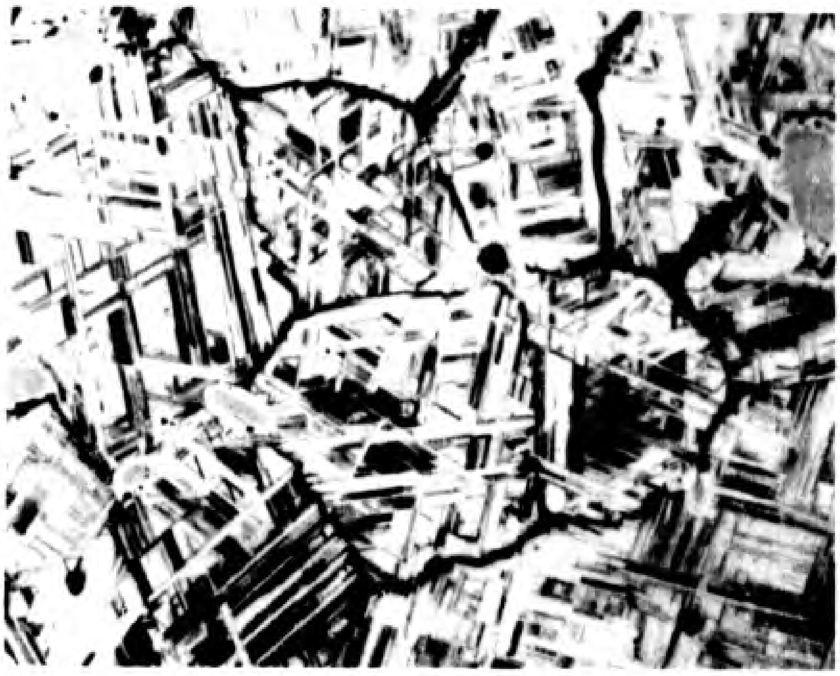

Figure 27. Nb-Mo-C (3-52-45 At.%), Cooled at Approximately 40°C per Second from 2500°C. X450

Incipient Decomposition in Molybdenum-Rich Monocarbide Grains, Surrounded by Small Amounts of Excess Graphite.

D. ASSEMBLY OF THE PHASE DIAGRAM

The experimental investigations of the solid state sections, combined with the results gained from DTA, melting point, and metallographic studies, have been used to construct the temperature sections shown in (Figures 28(a) through 28(h). In these illustrations, somewhat closer temperature spacings were employed in the vicinity of four-phase reaction planes to show more clearly the phases entering in, and emerging from, the principal and most important isothermal reactions occurring in the system.

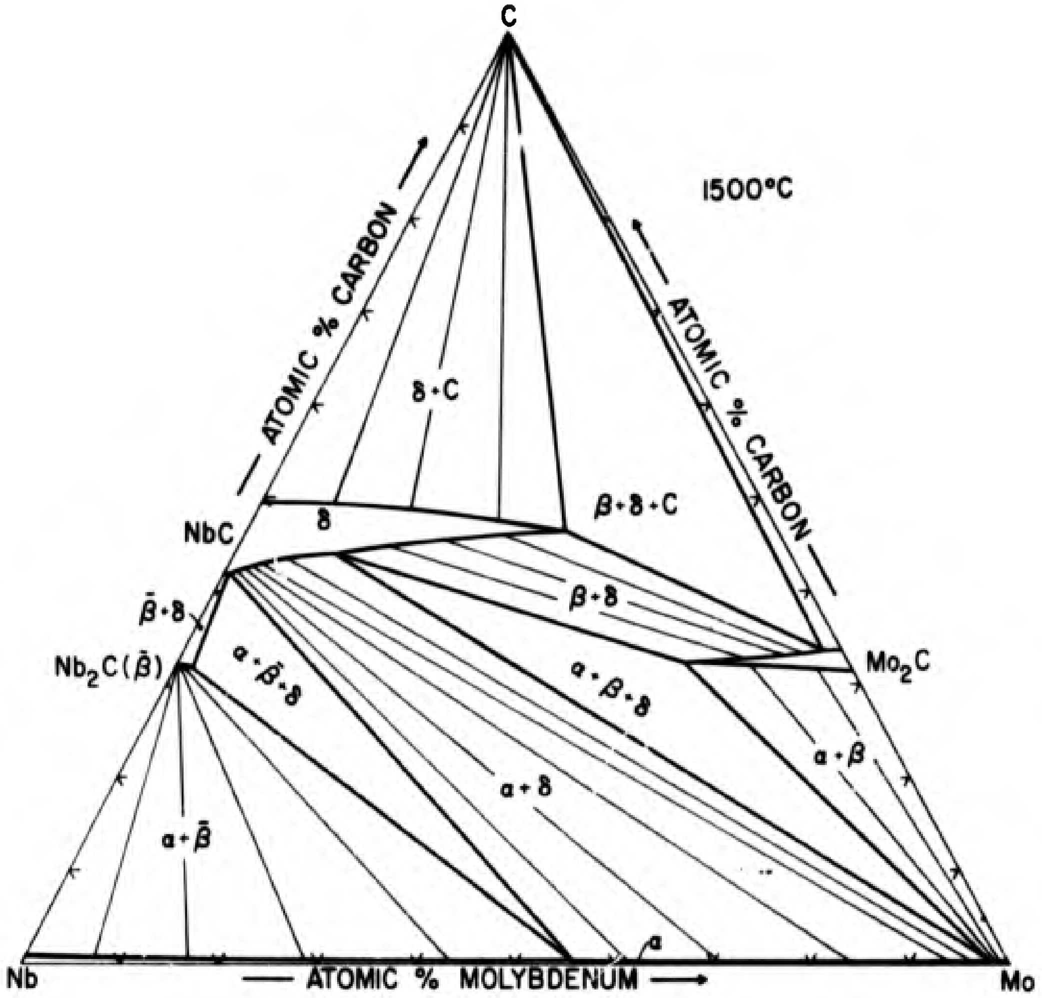

Figure 28(a). Isothermal Section at 1500°C.

Figures 28(a) through 28(h). Isothermal Sections for the Nb-Mo-C System.

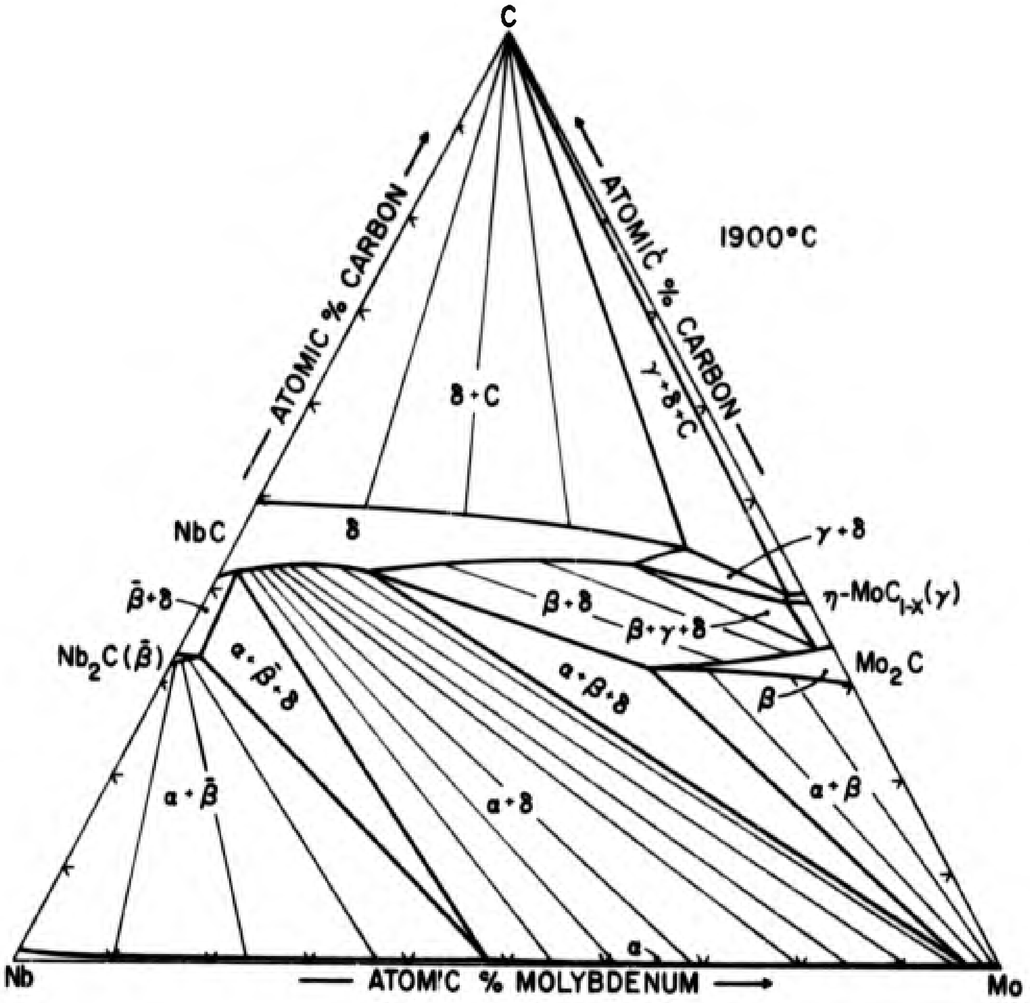

Figure 28(b). Isothermal Section at 1900°C

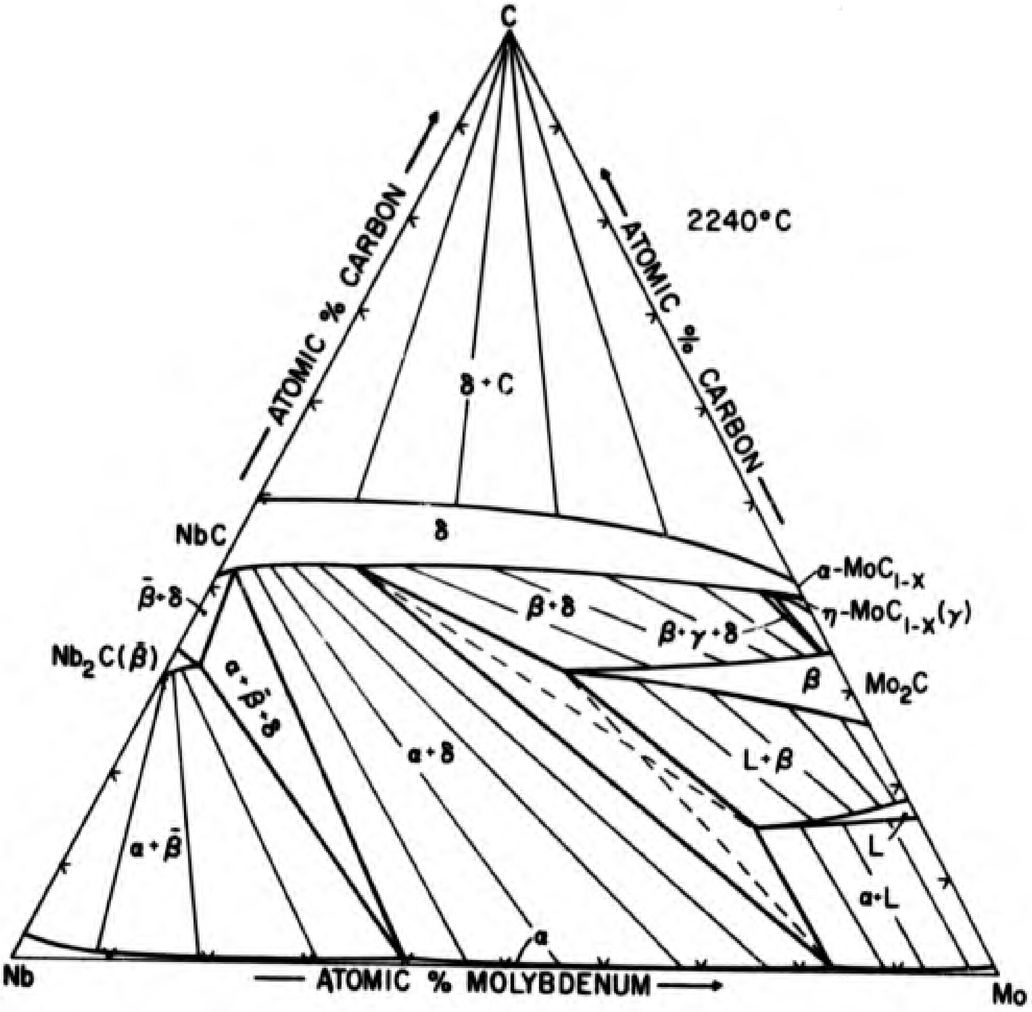

Figure 28(c). Isothermal Section at 2240°C

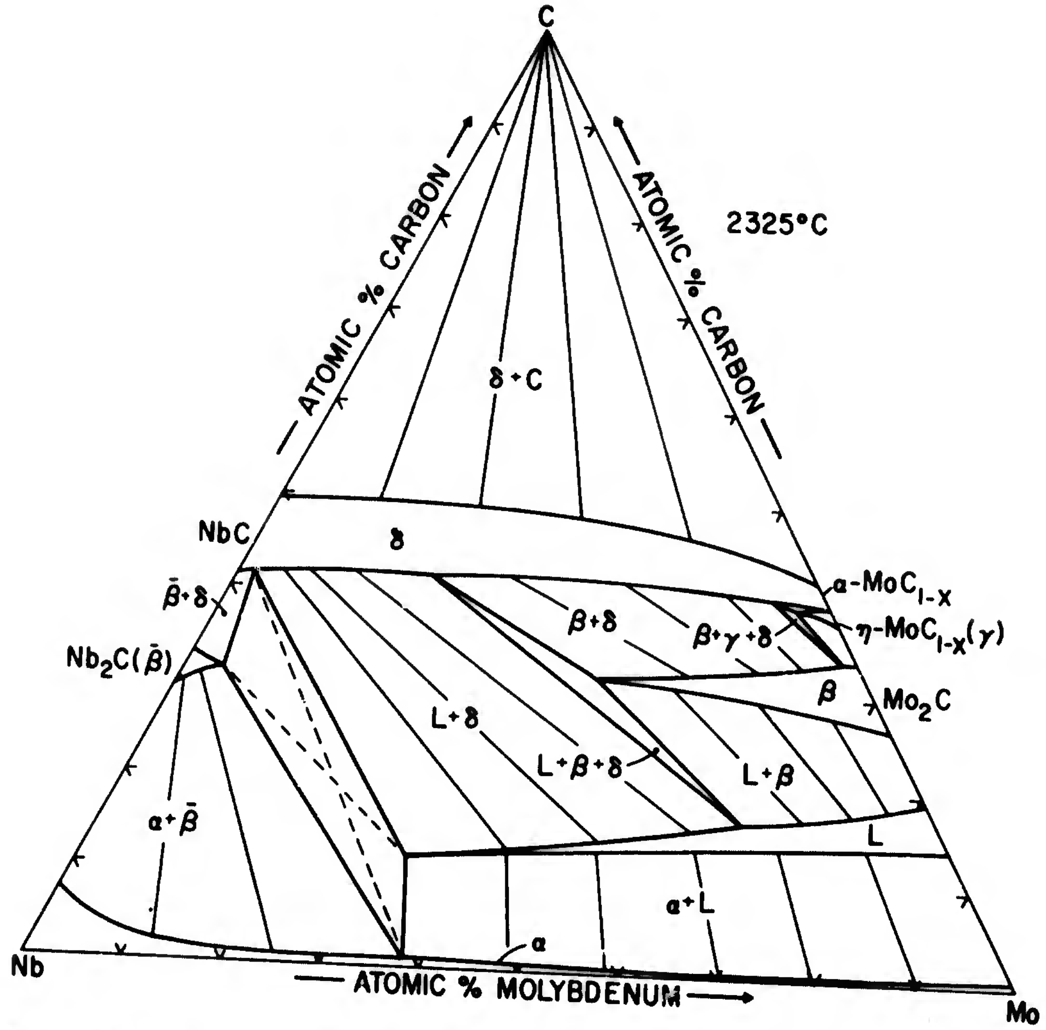

Figure 28(d). Isothermal Section at 2325°C

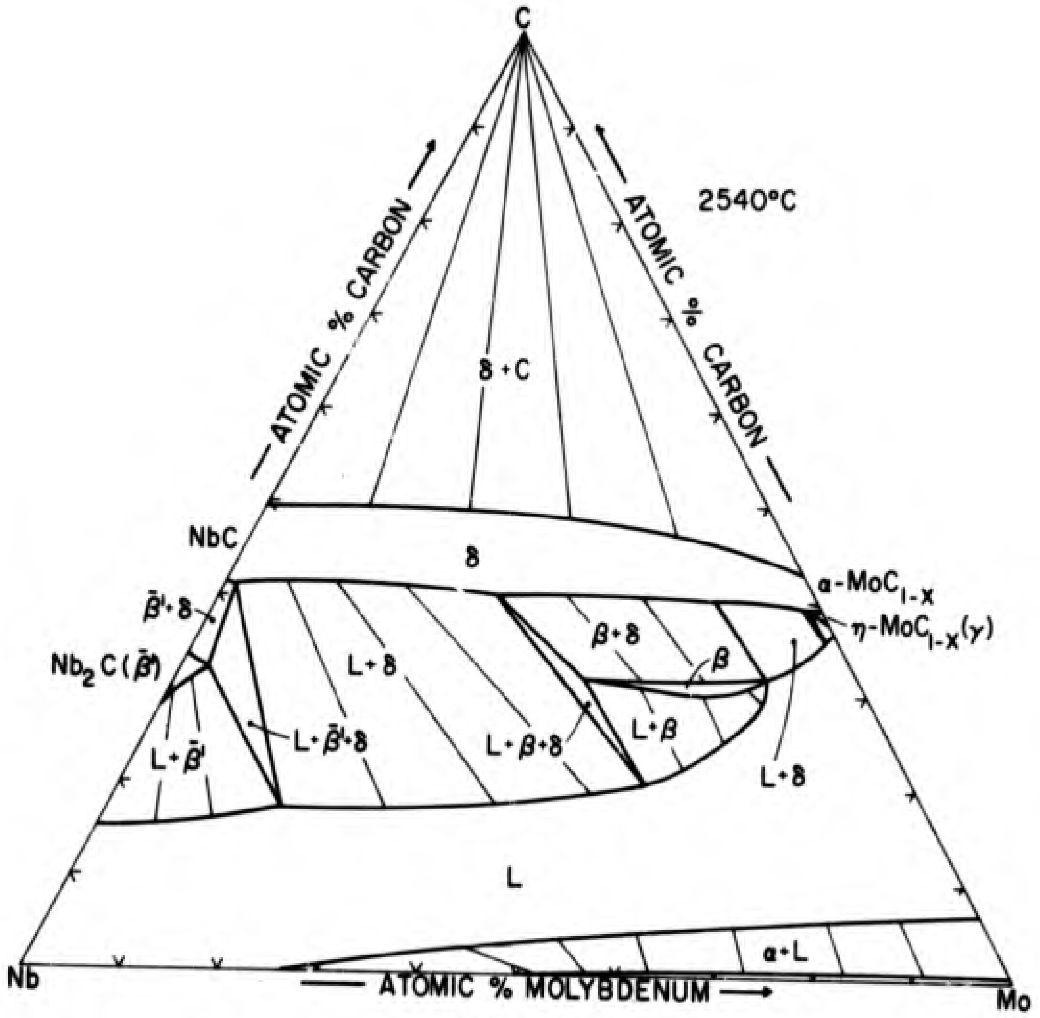

Figure 28(e). Isothermal Section at 2540°C

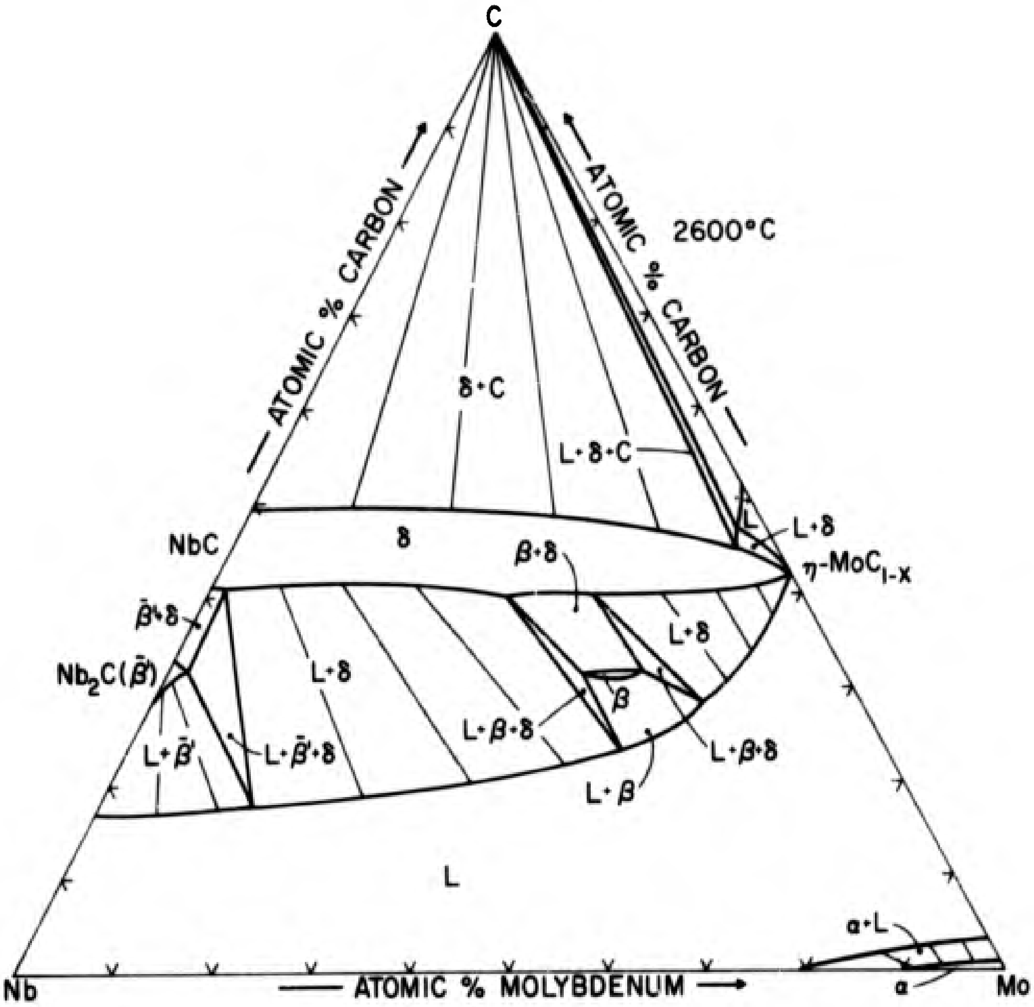

Figure 28(f). Isothermal Section at 2600°C

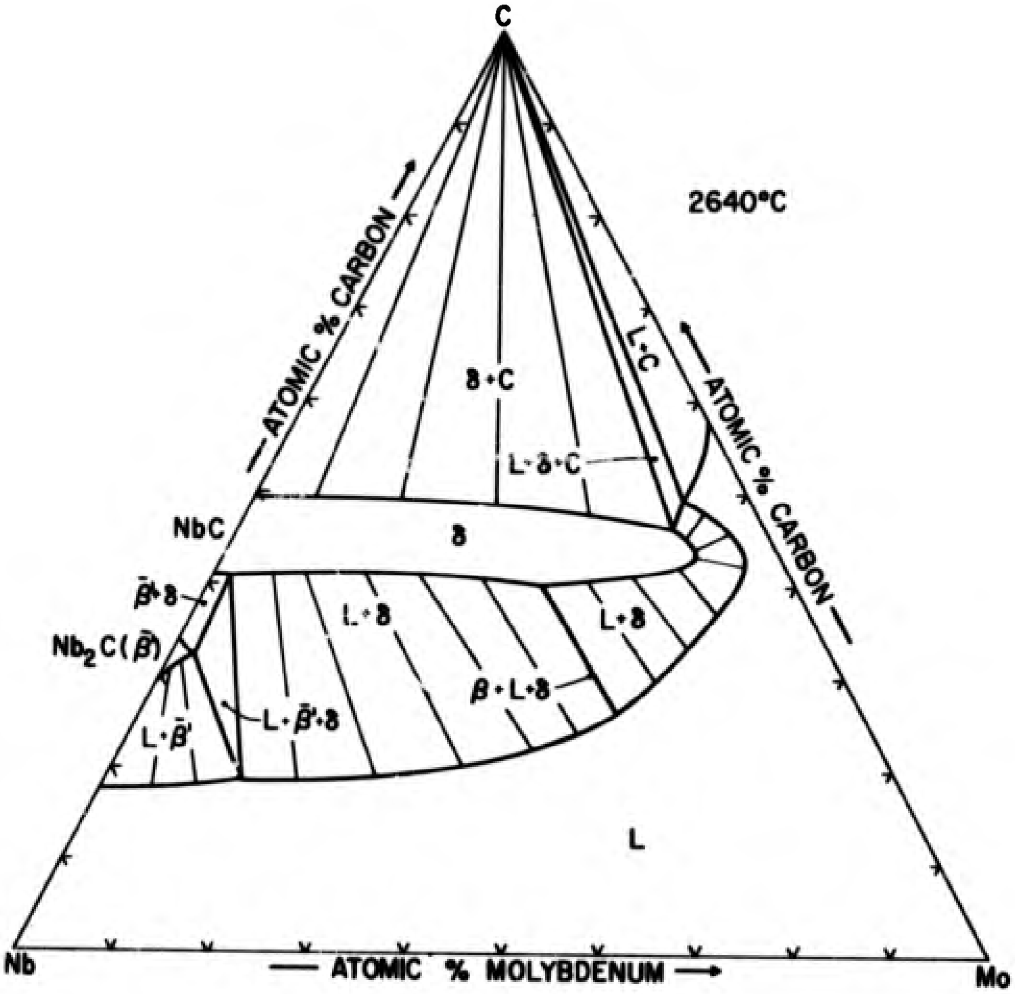

Figure 28(g). Isothermal Section at 2640°C

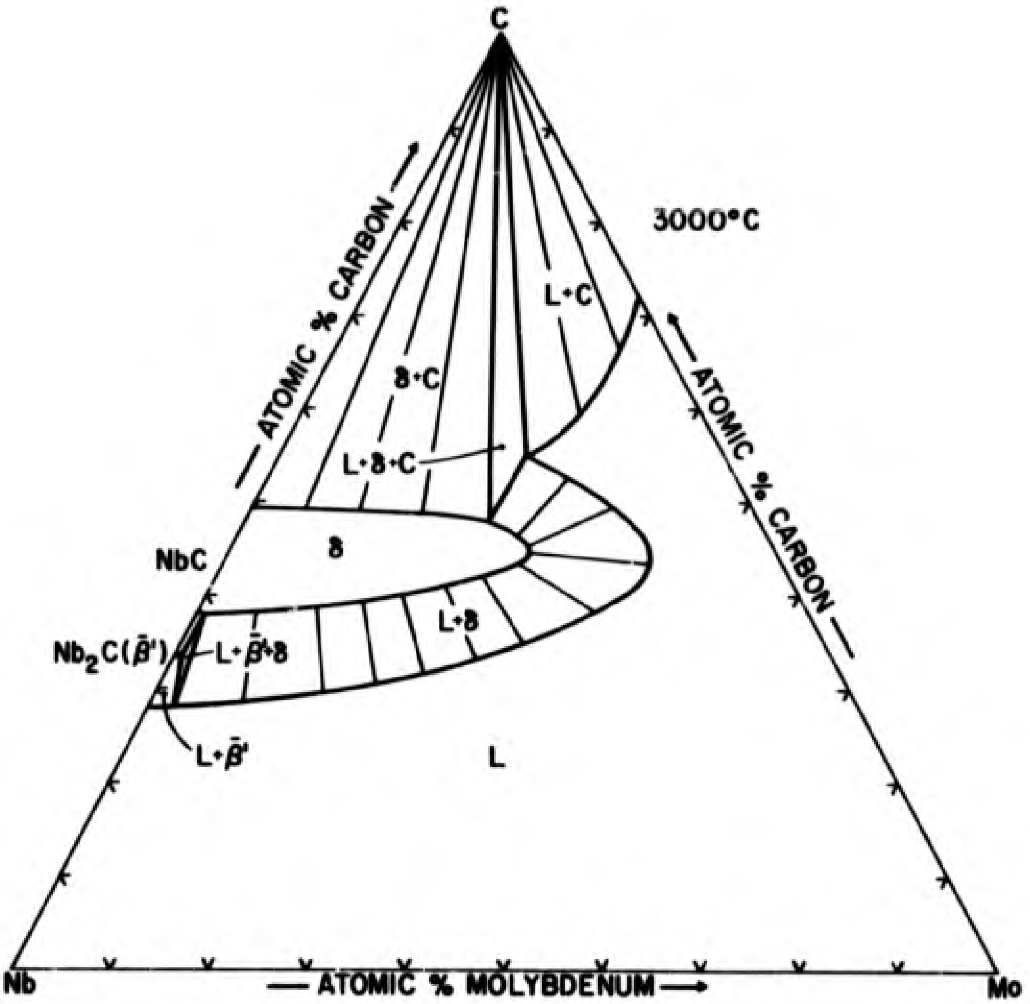

Figure 28(h). Isothermal Section at 3000°C

The appearance of the ζ-NbC_{1-x}-phase in the niobium-carbon system, occasionally observed(9), has been shown to be the result of a non-equilibrium precipitation from the defect monocarbide(11). Since, therefore, ζ-NbC_{1-x} is not regarded as a stable binary phase, and furthermore, was never observed in ternary alloys, it is not shown in the phase diagram.

The continuation of the order-disorder transformation of Nb_2C into the ternary is also not specifically shown in the section drawings, and hence, a short discussion is in order. DTA-studies on two stoichiometric subcarbide alloys containing three and five mole percent Mo_2C showed a small decrease in the transition temperatures from 2440°C for the binary phase, to approximately 2400°C in the ternary alloys. In slightly (0.8-1 At.% C) substoichiometric alloys, the temperatures of the phase transition are also lowered by molybdenum additions and decrease from approximately 2500°C, the maximum transition temperature in the binary Nb_2C, to approximately 2450°C in the terminal solid solution. However, because the reaction proceeds single-phased in substoichiometric alloys and is believed to be of higher order, these latter transformations were not regarded as true phase changes, and hence were not recorded in the phase diagram.

The carbon-rich boundary of the Nb_2C-phase retracts to metal-richer compositions upon molybdenum substitution, and the phase separation occurring in the binary system vanishes at 2480°C and 2 atomic percent molybdenum exchange in the ternary; in addition, a termination of the disordered, carbon-rich phase in a limiting tie line according to a reaction scheme;

$$Nb_2C\text{-ss (disordered)} \longrightarrow Nb_2C_{1-x}\text{-ss (ordered)} + (Nb,Mo)C_{1-x}\text{-ss}$$

at 2400°C was found to best account for the experimental observations.

The phase equilibrium relations below 1500°C were not specifically investigated, since prohibitively long annealing times would have been required to attain equilibrium. Two phase changes, however, which occur below 1500°C, will be discussed briefly, since some experimental data could be gathered by DTA-techniques. As discussed in earlier papers$^{(11, 12, 16)}$, Nb_2C undergoes a change in sublattice order at approximately 1230°C, whereas the stoichiometric Mo_2C-phase disproportionates below 1430°C into an ordered and a disordered phase. No noticeable change in the low temperature transition in Nb_2C was found upon substitution of molybdenum (Figure 16); this result is to be expected, because the solid solubilities in Nb_2C are very small at these temperatures. For Mo_2C, however, the mean transition temperatures decrease from 1430°C, for the binary compound, to approximately 1300°C for the terminal solid solution $\sim$22 mole% Nb_2C (Figure 16). From similar reasons as outlined from the high temperature transition in Nb_2C, the phase separation in Mo_2C ceases to exist at niobium exchanges of approximately

2-3 atomic percent. The temperature of the terminating tie line is indicated to be between 1400 and 1410°C. Since, therefore, the disordered β-Mo_2C-phase does not participate as a distinct entity in the three-phase equilibrium (Nb, Mo)-ss-$(Nb, Mo)C_{1-x}$-ss-Mo_2C-ss, and the transition in Nb_2C also does not involve a first order phase change, no further four-phase equilibria are expected to result from the order-disorder transitions in the subcarbides in the temperature range from 1200 to 1500°C.

Concerning the overall phase distribution for temperatures below 1500°C, no principal change of the major equilibria found at higher temperatures, is to be anticipated. However, as a result of the decrease of the positional free energy with decreasing temperature, the swing of the tie lines in the various two-phase fields will be more extreme than at the higher temperatures; also, the solid solubility ranges of the monocarbide and subcarbide phases will decrease somewhat with decreasing temperature.

In view of the difficulties in experimentally ascertaining the phase equilibria at low temperatures, it will be preferable and probably also more accurate, to use thermodynamic approaches for the determination of the coexisting phase compositions.

V. DISCUSSION

The most interesting feature in this system concerns the interruption of the solid solution series $(Nb, Mo)_2C$ by an equilibrium: monocarbide + metal phase. Similar equilibria between metal and monocarbide solutions have, in the meantime, also been found in other combinations of the group V with group VI metals and carbon, such as in the systems Ta-W-C, Ta-Mo-C, and Nb-W-C(1). In the corresponding systems with vanadium, however, the subcarbides form continuous series of solid solutions, i.e. two-phase equilibria, consisting of monocarbide and metal phase, do not exist in these systems.

In spite of the striking similarity of the lower temperature ($<2000°C$) phase relationships in the niobium and tantalum systems, their phase behavior becomes markedly different above 2000°C: In the systems Nb-W-C and Nb-Mo-C, the two-phase equilibria Me + MeC remain stable up to melting temperatures, whereas this equilibrium disappears in the systems Ta-Mo-C and Ta-W-C above approximately 2400°C as a result of complete solid solution formation between the subcarbides.

A thermodynamic analysis of the phase equilibria in the Ta-W-C system(3, 4) showed that the disproportionation of the subcarbide solution is due to the large stability differences between the carbides of tantalum and tungsten and to the relatively small free energies of disproportionation of the respective subcarbides. In order to discuss the disproportionation of the $(Nb,Mo)_2C$ solid solution on a thermodynamic basis, we consider an equilibrium between three solid solutions, viz.:

$$(A,B)C_u + (A,B)C_v + (A,B)C_w, \qquad (1)$$

where A stands for niobium, B for molybdenum, C for carbon, and the subscripts u, v, w are used to indicate the composition of the phases with respect to the component C.

Equilibrium (1) can be written as a disproportionation reaction ($u < v < w$) according to:

$$(w-u)\cdot(A,B)C_v \longrightarrow (w-v)\cdot(A,B)C_u + (v-u)\cdot(A,B)C_w \ldots \Delta G_Z,$$

where the free enthalpy change ΔG_Z is to be regarded as a measure of the stability of the interstitial phase solution $(A,B)C_v$ with respect to mechanical mixtures of solid solutions $(A,B)C_u$ and $(A,B)C_w$.

Generally speaking, the free enthalpies of the three, phase solutions will be a function of the relative metal exchange, (A, B), as well as the interstitial content (u, v, w); however, as shown previously(4, 26), for these types of interstitial compounds, not too serious an error is committed, if to a first approximation, u, v, w, are regarded as constant, i.e., if the free energy is allowed to change only by varying the relative metal content. Under these assumptions the stability condition for the equilibrium state can be written as:

$$(v-w)\bar{G}_{Z(u)} + (w-u)\bar{G}_{A(v)} + (u-v)\bar{G}_{A(w)} = 0 \qquad (2a)$$

or, the analogous equation for the component B:

$$(v-w)\bar{G}_{B(u)} + (w-u)\bar{G}_{B(v)} + (u-v)\bar{G}_{B(w)} = 0 \qquad (2b)$$

In these equations, the $\bar{G}_{A(i)}$ and $\bar{G}_{B(i)}$ are the partial molar free enthalpies of the components A and B in the phase solutions i (i = u, v, w). Using the binary phases at the respective semimetal concentrations (u, v, w) as the reference states, we may separate the partial free enthalpies into base and concentration-dependent terms, and obtain for the equilibrium case:

$$\Delta G_{ZAC_v} + \overline{\Delta G}^{mix}_{ZAC_v} = 0 \qquad (3a)$$

and

$$\Delta G_{ZBC_v} + \overline{\Delta G}^{mix}_{ZBC_v} = 0 \qquad (3b)$$

where ΔG_{ZAC_v} and ΔG_{ZBC_v} are the free enthalpies of disproportionation of the binary phases AC_v and BC_v according to:

$$(w-u)\,A(B)C_v \longrightarrow (w-v)\,A(B)C_u + (v-u)\,A(B)C_w \ldots \Delta G_{ZA(B)C_v},$$

and $\overline{\Delta G}^{mix}_{ZA(B)C_v}$ abbreviates the sum of mixing terms according to the above reaction scheme. The obvious meaning of equations (3a) and (3b) is that, under equilibrium conditions, the free enthalpies of disproportionation of the binary phases are exactly counterbalanced by the free energy of mixing in the three, phase solutions.

Any deviation from the equilibrium state will result in the appearance of a finite quantity, ϕ_Z, on the right hand side of equations (3), which essentially is a measure of the imbalance between the disproportionation terms for the binary phases and the mixing quantities. Generalizing conditions (3) we may write, therefore:

$$\phi_{Z(A)} = \Delta G_{ZAC_v} + \overline{\Delta G}^{mix}_{ZAC_v} , \tag{4a}$$

and

$$\phi_{Z(B)} = \Delta G_{ZBC_v} + \overline{\Delta G}^{mix}_{ZBC_v} . \tag{4b}$$

We note that, at equilibrium, $\phi_Z(x) = 0$; when $\phi_Z(x)$ assumes positive values, the solution $(A,B)C_v$ is stable with respect to mechanical mixtures of $(A,B)C_u$ and $(A,B)C_w$, whereas for $\phi_Z(x) < 0$, single phase solutions of $(A,B)C_v$ become unstable.

We further note that the equations satisfy the following boundary conditions:

$$\phi_{Z(A)}[x_{A(v)} = 1] = \Delta G_{ZAC_v}$$

$$\phi_{Z(A)}[x_{A(v)} = 0] = \Delta G_{ZBC_v}$$

$$\phi_{Z(B)}[x_{B(v)} = 1] = \Delta G_{ZBC_v}$$

$$\phi_{Z(B)}[x_{B(v)} = 0] = \Delta G_{ZAC_v}$$

So far, the relations discussed have dealt only with partial quantities. Knowing both partial disproportionation functions $\phi_{A(A)}$ and $\phi_{A(B)}$, the integral free enthalpy of disproportionation, $\phi_Z(x)$, of the solid solution $(A,B)C_v$ is given by:

$$\phi_Z(x) = x_{A(v)} \cdot \phi_{Z(A)} + x_{B(v)} \cdot \phi_{Z(B)} , \qquad (5)$$

where $x_{A(v)}$ and $x_{B(v)}$ are the mole fractions of the phases AC_v and BC_v, respectively. It could be shown(27) that both partial functions, $\phi_{Z(A)}$ and $\phi_{Z(B)}$, are identical, and, since $x_{A(v)} = 1 - x_{B(v)}$, are equal to the integral free enthalpy of disproportionation of the ternary phase solution $(A,B)C_v$, viz.,

$$\phi_Z(x) \equiv \phi_{Z(A)}(x_A) \doteq \phi_{Z(B)}(x_B) \qquad (6)$$

The stability of the ternary phase solution is therefore given by the partial free enthalpies of disproportionation of either of the two boundary phases; the Z-functions, as we will refer to the quantities $\phi_Z(x)$ later on, offer, therefore, a very convenient means of comparing the stability of a phase solution with those of mechanical mixtures of neighboring phase solutions.

In order to evaluate the above relations qualitatively, we have to know the free enthalpies of formation of the binary phases at the respective semimetal contents, as well as the compositions of the coexisting phases in the two-phase ranges adjoining the three-phase equilibria.

From the data compiled by E. K. Storms(28), H. L. Schick(29), and Y.A. Chang(30), as well as from values back-calculated from ternary phase diagrams(26, 31); we obtain the data listed in Table 4 for the niobium carbides, after linearization of the expressions. For the molybdenum carbides(16, 32), the data presented in Table 5 were used as the basis for the calculations.

Using the same assumptions, namely, constant semimetal contents of the phase solutions, the tie line distribution within the three, two-phase equilibria adjoining the three-phase range $(A,B)C_u + (A,B)C_v + (A,B)C_w$ is governed by the conditional equation(26) (T, p = const):

$$\left[\frac{\partial \Delta G_{f,(A,B)C_u}}{\partial x'}\right] = \left[\frac{\partial \Delta G_{f(A,B)C_v}}{\partial x''}\right] = \left[\frac{\partial \Delta G_{f,(A,B)C_w}}{\partial x'''}\right] , \qquad (7)$$

Table 4. Free Enthalpy Data of Niobium Carbides
(T > 1500°C)

Phase	Free Energy of Formation or Reaction (cal/gr.-At.Nb)
$NbC_{0.71}$-	$\Delta G_f = -27,350 + 0.0833 \cdot T$
$NbC_{0.75}$	$\Delta G_f = -28,250 + 0.807 \cdot T$
Disproportionation of $NbC_{0.485}$	$\Delta G_Z = 1982 - 0.54 \cdot T$

where x', x'', and x''' denote the relative mole fractions of A, or B, respectively, in the solid solutions $(A,B)C_u$, $(A,B)C_v$, and $(A,B)C_w$. Assuming, for the sake of simplicity, ideal behavior for the metal and subcarbide solid solutions, and describing the monocarbide phase as a regular solution with $\epsilon = 2000$ cal/gr.At. metal$^{(26)}$; we obtain, choosing the mole fraction of molybdenum as the concentration variable, the following conditional equations for the three, two phase ranges:

1. Two-Phase Equilibrium (Nb,Mo)-(Nb,Mo)$C_{0.485}$ ($u \sim 0$, $v \simeq 0.485$):

$$\log K_{1,2} = \frac{3652}{T} - 0.61 ,$$

where $K_{1,2}$ stands for

$$K_{1,2} = \frac{x'}{1-x'} \cdot \frac{1-x''}{x''}$$

Table 5. Free Enthalpy Data of Molybdenum Carbides
($T > 1500°C$)

Phase	Free Energy of Formation or Reaction (cal/gr.-At.Mo)
$MoC_{\sim 1/2}$	$\Delta G_f = -4,757 - 1.36 \cdot T$
η-MoC_{1-x} $(1-x \sim 0.64)$	$\Delta G_f \simeq -4,115 - 1.69 \cdot T$
α-MoC_{1-x} $(1-x \sim 0.70)$	$\Delta G_f \simeq -2,200 - 2.55 \cdot T$

2. Two-Phase Equilibrium (Nb, Mo)-(Nb,Mo)$C_{0.71}$ ($u \simeq 0$, $w \simeq 0.71$):

$$\log K_{1,3} = \frac{5597}{T} - 0.742 + \frac{438}{T}(1-2x''') ,$$

with

$$K_{1,3} = \frac{x'}{1-x'} \cdot \frac{1-x'''}{x'''}$$

3. Two-Phase Equilibrium (Nb, Mo)$C_{0.485}$-(Nb,Mo)$_{0.71}$ ($v=0.485$, $w=0.71$):

$$\log K_{2,} = \frac{1945}{T} - 0.132 + \frac{438}{T}(1-2x''')$$

where $K_{2,3}$ stands for the expression:

$$K_{2,3} = \frac{x''}{1-x''} \cdot \frac{1-x'''}{x'''}$$

Although the equations above could be solved analytically, the graphical evaluation is much more convenient, especially, since non-ideality terms also have to be considered. Thus, from the graphical plots of the gradient curves for the chosen equilibrium temperatures (Figures 29a through 29c), the coexisting phase compositions between any two phase combinations can be obtained from the horizontal intercepts (gradient = const) at any one prechosen set of concentrations.

Inserting the stoichiometry factors, u, v, w, into the equations (3a) and (3b), and writing down explicitly the solution terms, we obtain, after rearranging, for the Z-function of the solid solution $(\mathrm{Nb, Mo})\mathrm{C}_{\sim 1/2}$:

$$\phi_Z(x) = \phi_{Z\mathrm{NbC}_{\sim 1/2}} = \Delta G_{Z\mathrm{NbC}_{\sim 1/2}} = 2000\left(1 - x'''_{(\mathrm{Nb})}\right)^2 + RT \cdot \ln \frac{x'''^{\,0.658}_{(\mathrm{Nb})} \cdot x'^{\,0.342}_{(\mathrm{Nb})}}{x''_{(\mathrm{Nb})}} , \quad (8a)$$

or, the equivalent expression applying to $\mathrm{Mo_2C}$:

$$\phi_Z(x) = \phi_{Z\mathrm{MoC}_{\sim 1/2}} = \Delta G_{Z\mathrm{MoC}_{\sim 1/2}} + 2000\left(1 - x'''_{(\mathrm{Mo})}\right)^2 + RT \cdot \ln \frac{x'''^{\,0.658}_{(\mathrm{Mo})} \cdot x'^{\,0.342}_{(\mathrm{Mo})}}{x''_{(\mathrm{Mo})}} \quad (8b)$$

The equilibrium compositions at the metal and monocarbide solid solutions (x', x''') can be obtained for a series of preselected values of subcarbide compositions (x'') from the gradient curves, and $\phi_Z(x)$ is computed from relation (7a) or (7b).

Carrying out the detailed calculations, we obtained the curves shown in Figure 30. By definition, the intercepts at 0 and 100 atomic percent molybdenum correspond to the free enthalpies of disproportionation of the binary phases $\mathrm{NbC}_{\sim 1/2}$ and $\mathrm{MoC}_{\sim 1/2}$, respectively. As can be further seen from the graphical presentation of the Z-function for the subcarbide solution in Figure 30, the stability of the $\mathrm{Nb_2C}$-rich solid solution decreases rapidly upon incorporation of molybdenum into the lattice; the intercepts of the curves $\phi_Z(x)$ with the

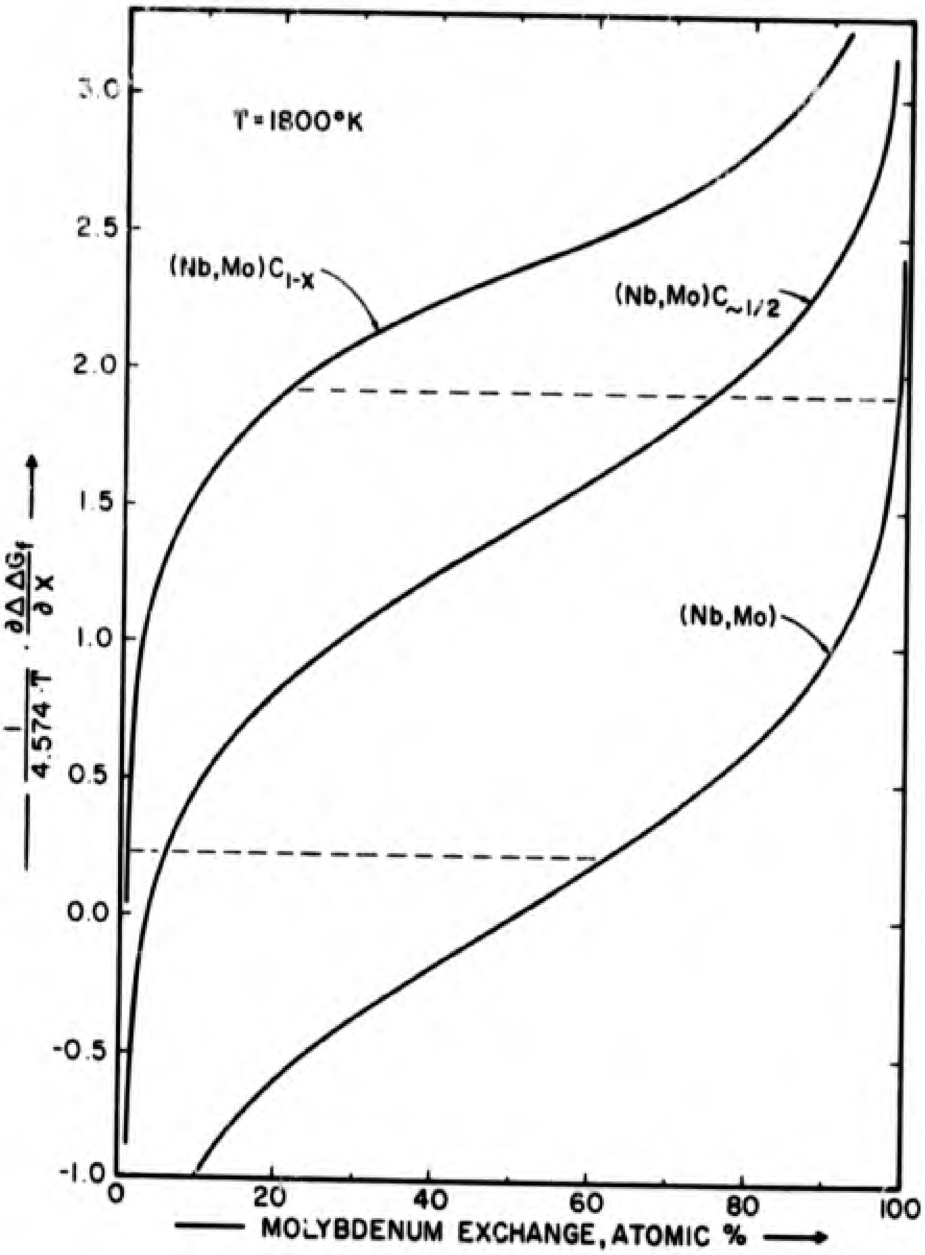

Figure 29(a). Free Enthalpy-Gradient Curves at 1800°K

Figures 29(a) through 29(c). Free Enthalpy of Formation — Concentration Gradients for Niobium-Molybdenum Alloys and Solutions of Niobium-Molybdenum Carbides.

(Dashed Lines: Phase Compositions Coexisting in Three-Phase Equilibria).

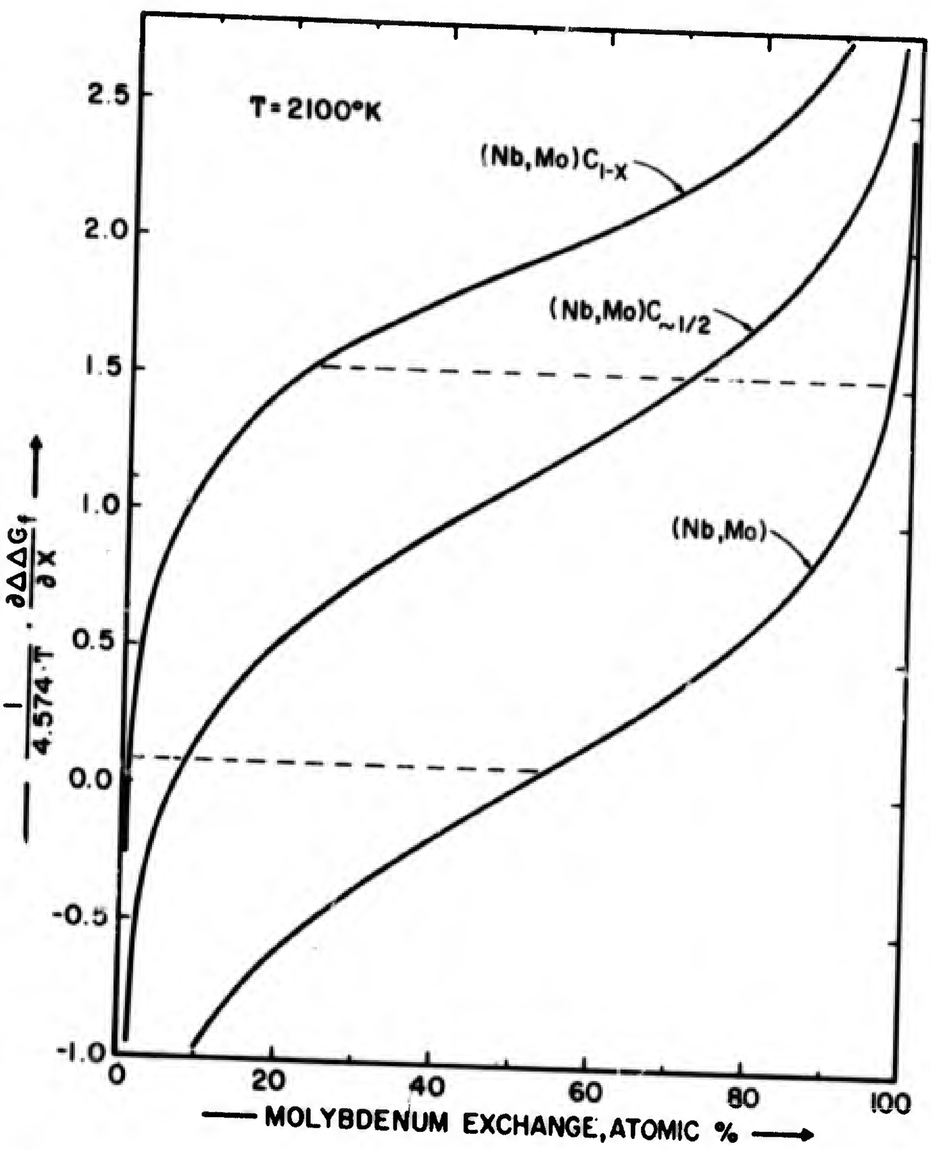

Figure 29(b) Free Enthalpy-Gradient Curves at 2100°K

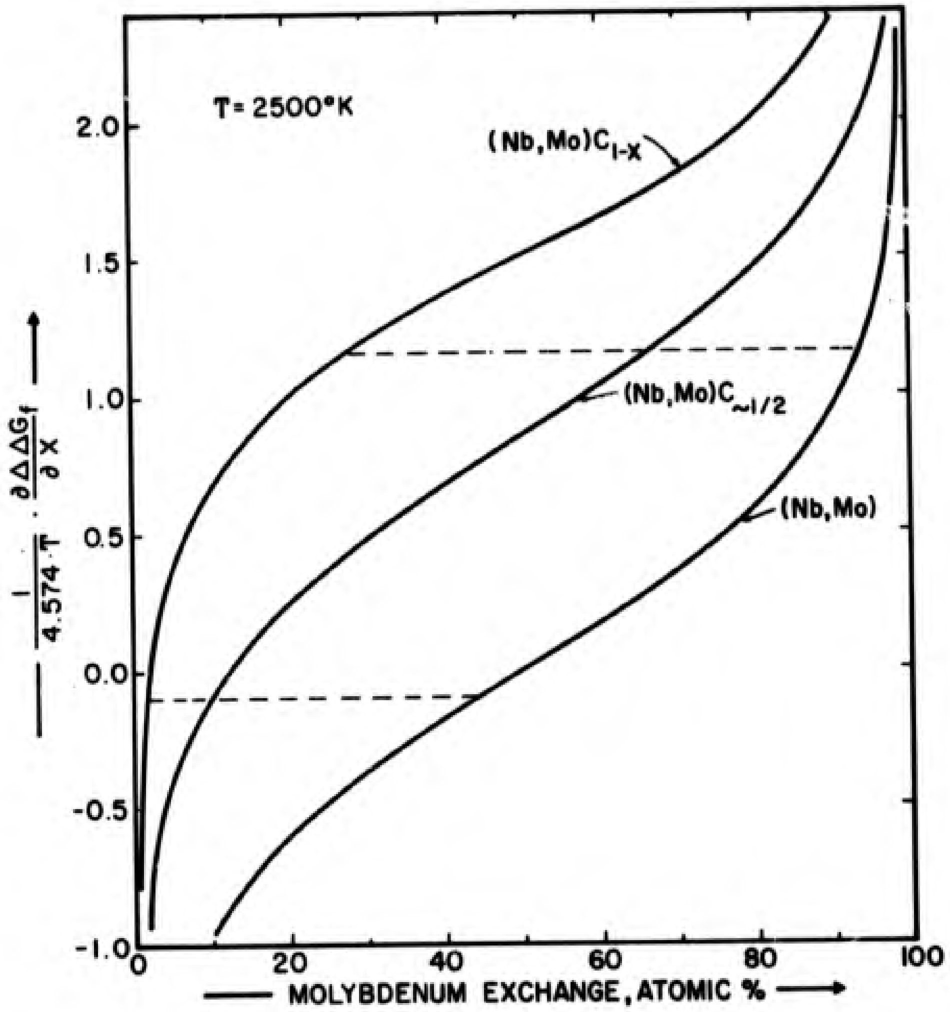

Figure 29(c). Free Enthalpy-Gradient Curves at 2500°K

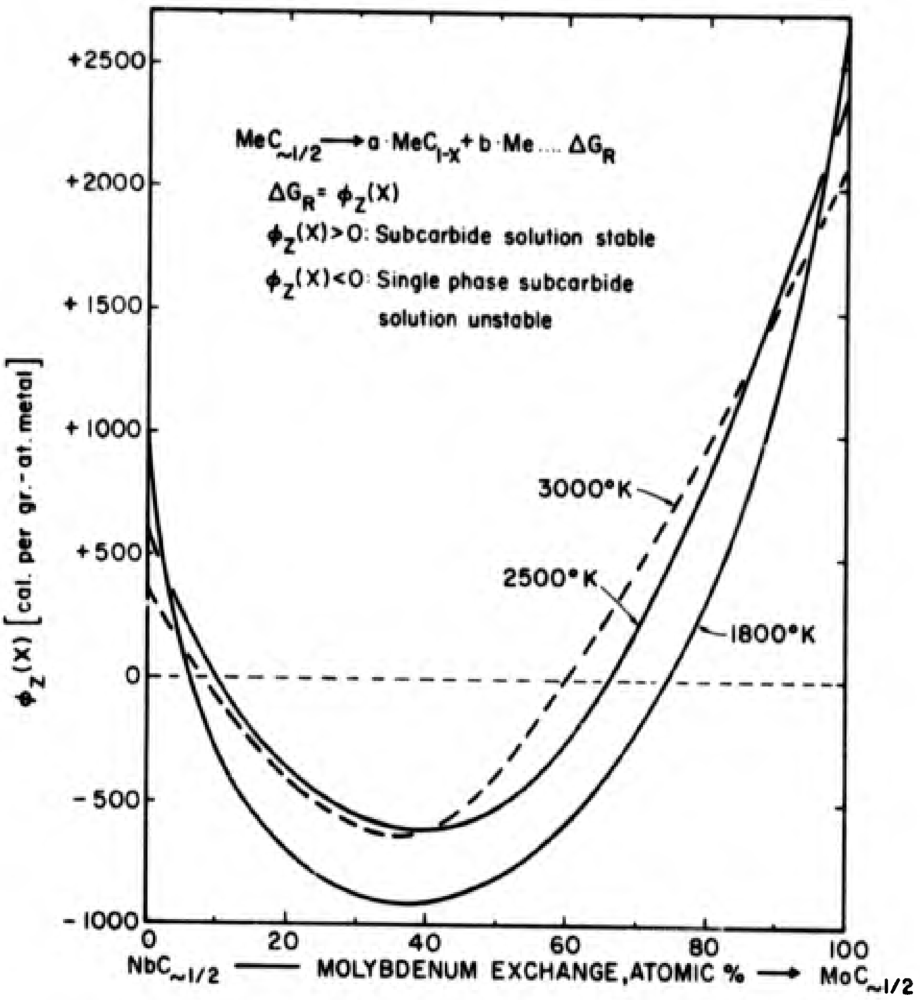

Figure 30. Calculated Integral Free Enthalpies for the Disproportionation of the Solid Solution $(Nb, Mo)_2C$ into (Nb, Mo) and $(Nb, Mo)_{1-x}$ Solid Solutions.

line $\phi_X(x) = 0$, which coincide with the stability limits of the Nb_2C-solid solution, lies at least 10 mole percent Mo_2C for all temperatures below solidus. Although hypothetical, the Z-function for the subcarbide solution calculated for 3000°K indicates that, even for the case that interference by the melt would not occur, a complete solid solution would still not be formed at high temperatures; in fact, due to the decreasing relative stability of Nb_2C, the solid solubility curve is expected to show even a retrograde behavior at higher temperatures. The minima of the Z-function lie in the vicinity of 40 atomic percent molybdenum; at the composition of the minimum at 1800°K, for example, the subcarbide solid solution is with approximately 900 calories unstable with respect to mechanical mixtures of monocarbide + metal phase; the relative stability of the subcarbide phase is only insignificantly affected by temperature changes.

According to the calculations, and in agreement with the experimental observations, the solid solubilities in Mo_2C are larger than in Nb_2C. This finding, on the one hand, has to be attributed to the higher relative stability of the binary Mo_2C, and on the other, to the large stability differences between niobium and molybdenum carbides, resulting in an extreme swing of the tie lines in the two-phase fields.

The other equilibria in the system to be considered, namely the three-phase equilibria $(Nb,Mo)C_{1-x}$-ss + η-MoC_{1-x}-ss + C, $(Nb,Mo)C_{1-x}$-ss + Mo_2C-ss + -MoC_{1-x}-ss, and $(Nb,Mo)C_{1-x}$-ss + Mo_2C-ss + C, can be evaluated by following the same procedures as above. Since the calculations are simple, but lengthy, they will not be described. With the vertices of the three-phase equilibria known, the individual phase fields in the system can be defined, and the coexisting phase compositions in the resulting two-phase fields obtained from the gradient curves. Three such temperature sections, at 1800°K, 2100°K, and 2500°K, have been calculated and are shown in Figures 31a through 31c.

Since, as a result of the assumptions made, only the relative metal exchanges are obtained from the calculations, no specific description of the

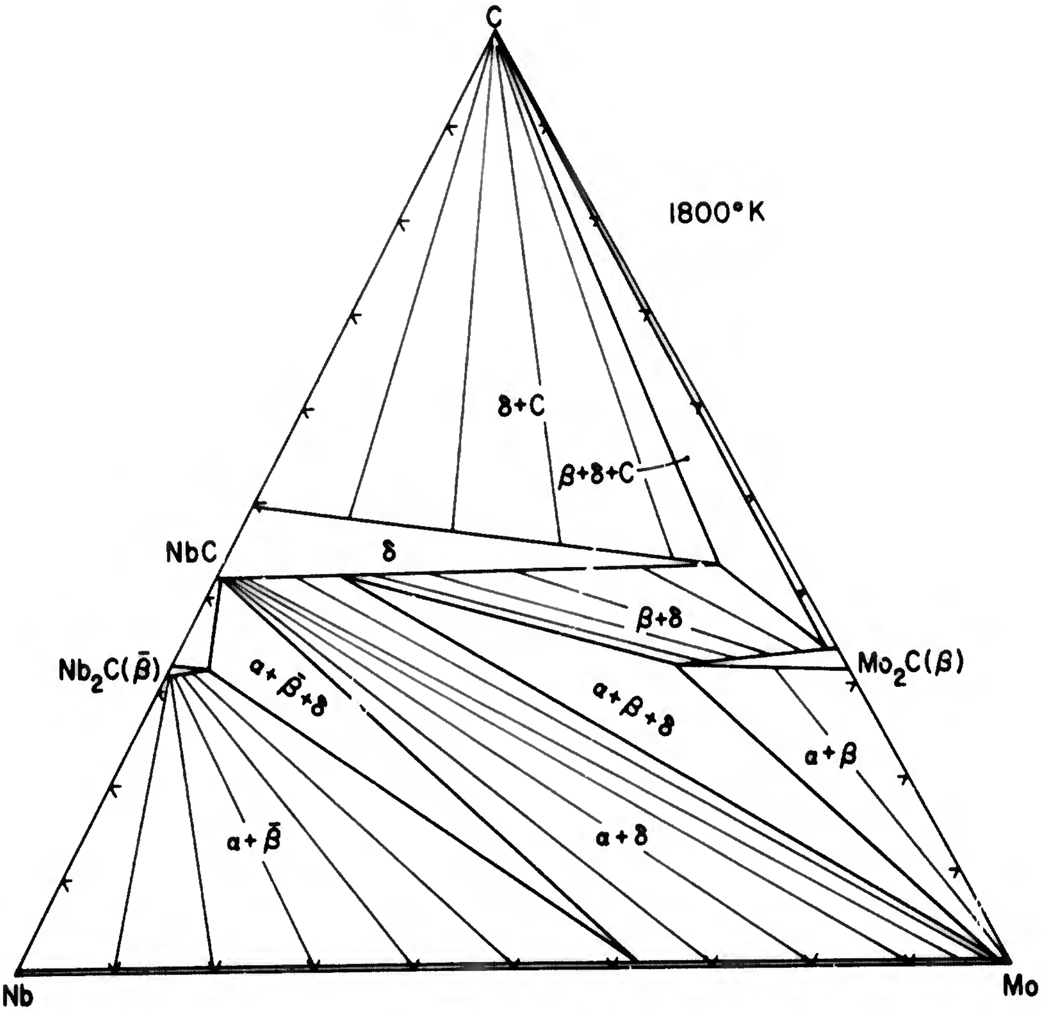

Figure 31(a). Calculated Section at 1800°K

Figures 31(a) through 31(c). Calculated Temperature Sections for the Nb-Mo-C System.

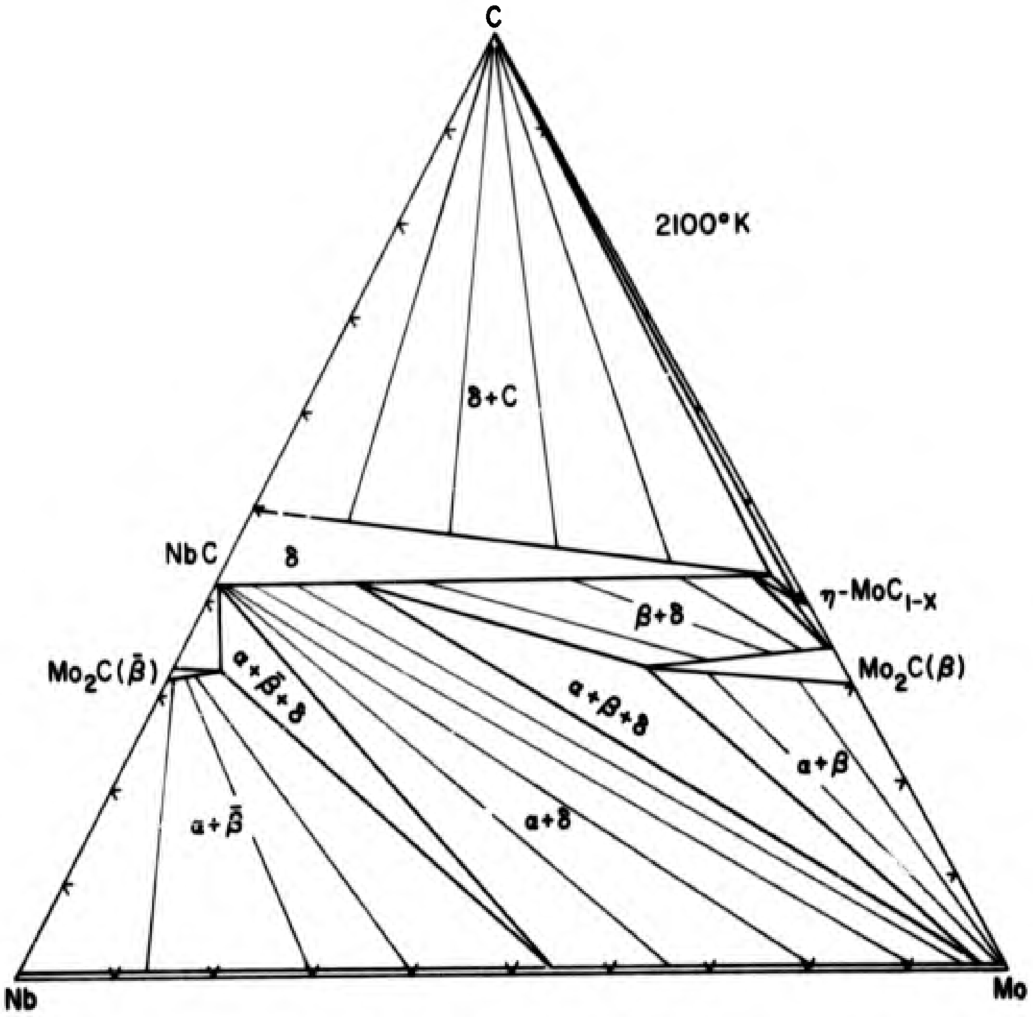

Figure 31(b). Calculated Section at 2100°K

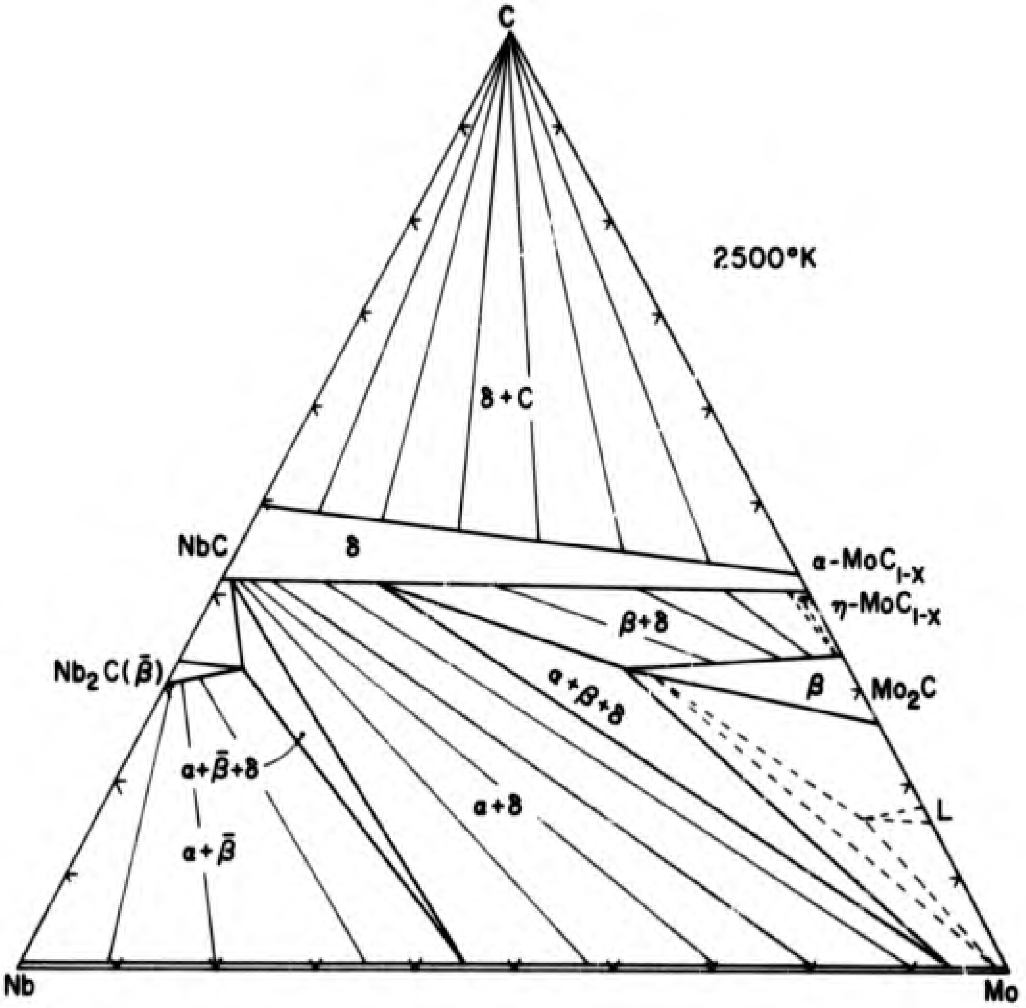

Figure 31(c). Calculated Section at 2500°K.

contours of the single-phase boundaries can be given; these boundaries, therefore, are shown as straight lines originating from the respective phase boundaries in the binary systems and terminating at the calculated vertices of the three-phase equilibria.

Considering the uncertainties of the thermodynamic data for the boundaries phases, as well as the simplifications made in the calculations, we note that agreement between the calculated and experimental phase relationships, especially for the equilibria in the metal-rich-region in the system, is exceedingly good. Major differences are encountered only for the monocarbide phase, where the calculated metal-exchanges are considerably larger than the experimentally determined solubilities. Part of these discrepancies are certainly attributable to the fact that the thermodynamic quantities submitted for the α-MoC_{1-x} refer only to a single composition (at ~40 At.% C); whereas, for the calculation of the ternary phase solution, the free enthalpy values of a cubic molybdenum carbide at a carbon content corresponding to that of the ternary solid solution would have to be employed. These data are not known, and a closer agreement between observed and calculated phase ranges could only be obtained by a trial and error fit of the equations to the experimental data, or by back-calculating pertinent datum points from the experimental phase diagram. However, since the primary objective of the present treatment was mainly to show the agreement between experimental and calculated phase relations by employing a straight-forward, first order approximation in the calculations and by using thermodynamic data available from the literature; this point will not be pursued at length. By the same token, a further refinement of the calculated phase equilibria along the lines outlined previously(4), and by using the present calculation as a first order approximation, would have to be based entirely upon assumed data for the free energy variations of the phase solutions, and would, therefore, also be reduced to a mere data fit. A simple consideration shows, furthermore, that for this system the changes to be expected from a more refined treatment would be small indeed.

REFERENCES

1. Work conducted under U.S. Air Force Contract AF 33(615)-1249, at the Materials Research Laboratory, Aerojet-General Corporation, Sacramento, California (Report Series AFML-TR-65-2, Part I to IV., 28 Volumes, 1964 to 1966).

2. E. Rudy, F. Benesovsky, and K. Sedlatschek: Mh.Chem., 1961, Vol. 92, p.841.

3. E. Rudy, El. Rudy, and F. Benesovsky: Mh. Chem., 1962, Vol. 93, p.1176.

4. E. Rudy: U.S. Air Force Contract AF 33(615)-1249, Report AFML-TR-65-2, Part II, Vol. VIII, March 1966 (to be submitted for publication in Trans. AIME).

5. H. Bückle: Z. Metallkde, 1946, Vol. 37, p.53.

6. H. Braun, K. Sedlatschek, and B.F. Kieffer: Planseeber.Pulvermet. 1960, Vol.8, p.58.

7. I.I. Kornilov and R.S. Polyakova: Trans.Akad. Nauk SSSR, 1957, Vol. 2, p. 149.

8. R.P. Elliott: Constitution of Binary Alloys, First Supplement, (McGraw-Hill, New York, 1965).

9. E.K. Storms and N.H. Krikorian: J.Phys.Chem., 1960,Vol.64, p.1471.

10. H. Kimura and Y. Sasaki: Trans.Japan Inst.Metals, 1961, Vol.2,p.98.

11. E. Rudy and St. Windisch: Planseeber. Pulvermetallurgie, 1967, (in print).

12. E. Rudy and C.E. Brukl: J.Amer.Ceram.Soc., 1967 (in print).

13. N. Terao: J.J.Appl.Phys., 1964, Vol.3, p.104.

14. E. Rudy and D.P. Harmon: Air Force Report AFML-TR-65-2, Part I, Vol. V (Jan 1966).

15. E. Rudy, St. Windisch, and Y.A. Chang: Air Force Report AFML-TR-65-2, Part I, Vol. I, (Jan 1965).

16. E. Rudy, St. Windisch, A.J. Stosick, and J.R. Hoffman (Submitted for publication in Trans. AIME).

17. H. Nowotny and R. Kieffer: Metallforschung 1947, Vol.2, p.257.

REFERENCES (Cont'd)

18. K. Yvon, H. Nowotny, and R. Kieffer: Mh. Chem., 1967, (to be published).

19. H. Nowotny, E. Parthe', R. Kieffer, and F. Benesovsky: Mh.Chem. 1954, Vol.85, p.255.

20. G. Brauer and R. Lesser: Z. Metallkde, 1959, Vol. 50, p.8.

21. E. Parthe' and V. Sadagopan: Acta. Cryst, 1963, Vol. 16, p.202.

22. W.B. Pearson: Handbook of Lattice Spacings and Structures of Metals, Pergamon Press, New York, 1958.

23. M. Pirani and H. Alterthum: Z. Elektrochem., 1923, Vol. 29, p.5.

24. E. Rudy and G. Progulski: Planseeber. Pulvermetallurgie, 1967 (in print).

25. H.D. Heetderks, E. Rudy, and T. Eckert: Planseeber Pulvermetallurgie, 1965, Vol.13, p.105.

26. E. Rudy: Z.Metallkde 1963, Vol. 54, p.112.

27. E. Rudy: Contract AF 33(615)-1249, U.S. AF Report AFML-TR-65-2, Part IV, Vol. II (Jan 1966).

28. E.K. Storms: Refractory Carbides (Academic Press, 1967, in print).

29. H.L. Schick: Thermodynamics of Certain Refractory Compounds, Vol. II (Academic Press, 1966).

30. Y.A. Chang: U.S. Air Force Contract AF 33(615)-1249, Report AFML-TR-65-2, Part IV, Vol. I (Sept 1965).

31. E. Rudy and Y.A. Chang: Plansee Proc. 1965, p.786 (Springer Wien-New York, 1965).

32. L.B. Pankratz, W.W. Weller, and E.G. King: U.S. Bureau Mines Report of Invest. No. 6861 (1966).

DOCUMENT CONTROL DATA - R&D

(Security classification of title, body of abstract and indexing annotation must be entered when the overall report is classified)

1. ORIGINATING ACTIVITY *(Corporate author)*
Materials Research Laboratory
Aerojet-General Corporation
Sacramento, California

2a. REPORT SECURITY CLASSIFICATION
Unclassified

2b. GROUP
N/A

3. REPORT TITLE
Ternary Phase Equilibria in Transition Metal-Boron-Carbon Silicon Systems
Part II. Ternary Systems. Vol. XV. Constitution of Niobium-Molybdenum-Carbon Alloys

4. DESCRIPTIVE NOTES *(Type of report and inclusive dates)*

5. AUTHOR(S) *(Last name, first name, initial)*
Rudy, Erwin
Brukl, Charles E.
Windisch, Stefan

6. REPORT DATE
July 1967

7a. TOTAL NO. OF PAGES
67

7b. NO. OF REFS
32

8a. CONTRACT OR GRANT NO. AF 33(615)-1249

b. PROJECT NO. 7350

c. Task No. 735001

d.

9a. ORIGINATOR'S REPORT NUMBER(S)
AFML-TR-65-2
Part II. Volume XV

9b. OTHER REPORT NO(S) *(Any other numbers that may be assigned this report)*
N/A

10. AVAILABILITY/LIMITATION NOTICES This document is subject to special export controls and each transmittal to foreign governments or foreign nationals may be made only with prior approval of the Air Force Materials Laboratory (MAM), Wright-Patterson Air Force Base, Ohio.

11. SUPPLEMENTARY NOTES

12. SPONSORING MILITARY ACTIVITY
AFML (MAMC)
Wright-Patterson AFB, Ohio 45433

13. ABSTRACT

The ternary alloy system niobium-molybdenum-carbon was investigated by means of X-ray, melting point, DTA, and metallographic techniques; a complete phase diagram for temperatures above 1500°C was established.

Above 1960°C, niobium monocarbide and the cubic (B1) high temperature phase in the molybdenum-carbon system form an uninterrupted series of solid solutions. The ternary range of the pseudo-cubic η-Mo_{1-x} is very restricted. Dimolybdenum carbide dissolves up to 44 mole percent Nb_2C (2240°C), whereas the maximum solid solubility of Mo_2C in Nb_2C does not exceed 5 mole percent. The order-disorder transformation temperatures in Mo_2C and Nb_2C are lowered by the mutual metal exchanges.

Six isothermal reactions occur in the ternary system; three correspond to class II-type four-phase reactions involving a liquid phase, one to a class I (eutectoid)-type, and two further isotherms are associated with limiting tie lines.

The results of the phase diagram investigation are discussed, and the thermodynamic interpretation identifies the low relative stability of the binary subcarbides in conjunction with the large stability differences between niobium and molybdenum carbides as the cause for the formation of a stable equilibrium between the monocarbide and the metal phase in the ternary region.

14. KEY WORDS	LINK A		LINK B		LINK C	
	ROLE	WT	ROLE	WT	ROLE	WT
Ternary Phase Equilibria Niobium-Molybdenum-Carbon Alloys Thermodynamics of Phase Reactions						

INSTRUCTIONS

1. ORIGINATING ACTIVITY: Enter the name and address of the contractor, subcontractor, grantee, Department of Defense activity or other organization *(corporate author)* issuing the report.

2*a*. REPORT SECURITY CLASSIFICATION: Enter the overall security classification of the report. Indicate whether "Restricted Data" is included. Marking is to be in accordance with appropriate security regulations.

2*b*. GROUP: Automatic downgrading is specified in DoD Directive 5200.10 and Armed Forces Industrial Manual. Enter the group number. Also, when applicable, show that optional markings have been used for Group 3 and Group 4 as authorized.

3. REPORT TITLE: Enter the complete report title in all capital letters. Titles in all cases should be unclassified. If a meaningful title cannot be selected without classification, show title classification in all capitals in parenthesis immediately following the title.

4. DESCRIPTIVE NOTES: If appropriate, enter the type of report, e.g., interim, progress, summary, annual, or final. Give the inclusive dates when a specific reporting period is covered.

5. AUTHOR(S): Enter the name(s) of author(s) as shown on or in the report. Enter last name, first name, middle initial. If military, show rank and branch of service. The name of the principal author is an absolute minimum requirement.

6. REPORT DATE: Enter the date of the report as day, month, year; or month, year. If more than one date appears on the report, use date of publication.

7*a*. TOTAL NUMBER OF PAGES: The total page count should follow normal pagination procedures, i.e., enter the number of pages containing information.

7*b*. NUMBER OF REFERENCES: Enter the total number of references cited in the report.

8*a*. CONTRACT OR GRANT NUMBER: If appropriate, enter the applicable number of the contract or grant under which the report was written.

8*b*, 8*c*, & 8*d*. PROJECT NUMBER: Enter the appropriate military department identification, such as project number, subproject number, system numbers, task number, etc.

9*a*. ORIGINATOR'S REPORT NUMBER(S): Enter the official report number by which the document will be identified and controlled by the originating activity. This number must be unique to this report.

9*b*. OTHER REPORT NUMBER(S): If the report has been assigned any other report numbers *(either by the originator or by the sponsor)*, also enter this number(s).

10. AVAILABILITY/LIMITATION NOTICES: Enter any limitations on further dissemination of the report, other than those imposed by security classification, using standard statements such as:

(1) "Qualified requesters may obtain copies of this report from DDC."

(2) "Foreign announcement and dissemination of this report by DDC is not authorized."

(3) "U. S. Government agencies may obtain copies of this report directly from DDC. Other qualified DDC users shall request through
_______________________________."

(4) "U. S. military agencies may obtain copies of this report directly from DDC. Other qualified users shall request through
_______________________________."

(5) "All distribution of this report is controlled. Qualified DDC users shall request through
_______________________________."

If the report has been furnished to the Office of Technical Services, Department of Commerce, for sale to the public, indicate this fact and enter the price, if known.

11. SUPPLEMENTARY NOTES: Use for additional explanatory notes.

12. SPONSORING MILITARY ACTIVITY: Enter the name of the departmental project office or laboratory sponsoring *(paying for)* the research and development. Include address.

13. ABSTRACT: Enter an abstract giving a brief and factual summary of the document indicative of the report, even though it may also appear elsewhere in the body of the technical report. If additional space is required, a continuation sheet shall be attached.

It is highly desirable that the abstract of classified reports be unclassified. Each paragraph of the abstract shall end with an indication of the military security classification of the information in the paragraph, represented as *(TS)*, *(S)*, *(C)*, or *(U)*.

There is no limitation on the length of the abstract. However, the suggested length is from 150 to 225 words.

14. KEY WORDS: Key words are technically meaningful terms or short phrases that characterize a report and may be used as index entries for cataloging the report. Key words must be selected so that no security classification is required. Identifiers, such as equipment model designation, trade name, military project code name, geographic location, may be used as key words but will be followed by an indication of technical context. The assignment of links, rules, and weights is optional.